Review Article

Secretory leukocyte peptidase inhibitor and lung cancer

Toshihiro Nukiwa,[1] Takuji Suzuki, Tatsuro Fukuhara and Toshiaki Kikuchi

Department of Respiratory Medicine, Tohoku University Graduate School of Medicine, 2-1 Seiryo-machi, Aoba-ku, Sendai 980-8575, Japan

(Received August 30, 2007/Revised January 15, 2008/Accepted January 16, 2008/Online publication March 28, 2008)

Secretory leukocyte peptidase inhibitor (SLPI) belongs to the whey acidic protein four-disulfide core family of proteins, and has antimicrobial and antiprotease functions. SLPI is produced by the epithelial cells lining the respiratory, digestive, and reproductive tracts. Gene-targeting experiments in mice indicated that one function of SLPI is to protect proepithelin from elastase cleavage in wound healing. In addition to its antiprotease function, SLPI has an anti-inflammatory function through the modulation of nuclear factor-κB acting intracellularly, especially in macrophages. SLPI is also produced in cancer tissues, but its role in cancer is not well understood. SLPI genes are often upregulated under tumorigenic conditions. We found a negligible number of tumors in the lungs of SLPI knockout mice 20 or 40 weeks after administration of urethane, an interesting experimental model for investigating the function of SLPI in cancer. This review discusses the normal function of SLPI and its possible roles in cancer tissues. (*Cancer Sci* 2008; 99: 849–855)

Secretory leukocyte peptidase inhibitor (SLPI), previously known as secretory leukoprotease (or leukocyte protease) inhibitor or antileukoproteinase, was originally isolated from the secretions of patients with chronic obstructive pulmonary disease in the 1970s and consists of 107 amino acids (11.7 kDa) organized in a duplicated, boomerang-shaped whey acidic protein four-disulfide core (WFDC) domain (Fig. 1).[1,2] SLPI is secreted from mucosal epithelial cells lining the respiratory, digestive, and reproductive tracts, as well as from neutrophils and macrophages.[3,4] It is highly expressed in the normal lung. According to the microarray data deposited in the National Centre for Biotechnology Information Gene Expression Omnibus (GEO; GSE1643), SLPI mRNA is among the most abundant transcripts, including those of surfactant proteins.[5] The lung epithelial lining fluid contains approximately 10 μM SLPI protein.[1] However, the SLPI protein is measured using lining fluid from respiratory, digestive, and genital organs, whereas the SLPI mRNA transcripts are determined using whole organs. In this context, the most recent reference of the relative expression of the SLPI mRNA transcript will come from GSE3526 (comparison of gene expression profiles across the normal human body) deposited by Dr RB Roth (Neurocrine Biosciences, Inc.) in 2005. The relative SLPI mRNA expression is high in trachea, bronchus, oral mucosa, salivary gland pharyngeal mucosa, esophagus, lung, and vagina (Table 1).

In addition, SLPI is expressed in cancer cells originating from organs that normally express SLPI. SLPI is upregulated in non-small cell lung cancer (NSCLC), and cancers of the ovary, cervix, and pancreas, but not in those of the breast, kidney, intestinal tract, or nasopharynx.[6] For example, SLPI is one of the six genes in pancreas cancer identified as being highly expressed by U133 oligonucleotide array, cDNA microarray, and serial analysis of gene expression (SAGE).[7] The function of SLPI expression in cancer tissues is not clear. As cancer tissues are sites of inflammation, consisting of cancer cells and mesenchymal stromal cells, SLPI may have a role in the formation of cancer tissues. Interestingly, the function of SLPI is not restricted to that of a protease inhibitor as originally defined. Recent reports have described distinct roles in immune and inflammatory modulation.[2,8] We attempted to establish urethane-based chemical carcinogenesis in the lungs of SLPI knockout mice, and found that lung carcinogenesis is suppressed in the absence of SLPI. The present review article provides an overview of the current understanding of the function of SLPI and discusses the role of SLPI in lung carcinogenesis.

Secretory leukocyte peptidase inhibitor as a whey acidic protein motif protein: Cloning, chromosome location, and regulation of tissue expression

To further investigate the function of SLPI in the lungs, we first cloned mouse SLPI mRNA from the lung poly A^+ RNA of C57BL/6 mice using degenerate primers based on human *SLPI* gene sequences, a region that is highly homologous with porcine SLPI.[9] The full-length mouse *SLPI* cDNA had 66% nucleotide homology and 58% amino acid homology with human SLPI. The tissue distribution of the SLPI mRNA transcripts in the mouse revealed high levels of expression in the lungs, spleen, small intestine, and epididymis, and low levels of expression in the liver and seminal vesicles.[9] We have identified a lung cell-specific region in the promoter of the human *SLPI* gene.[10] We examined the regulation of SLPI expression in the lungs of mice with pneumonia, and found that the SLPI transcript levels were upregulated by three-fold 10 h after nasal inoculation with *Streptococcus pneumoniae*.[9]

Secretory leukocyte peptidase inhibitor is located on chromosome 20q12–13.1 in humans and on chromosome 2H in mice with a similar exon–intron configuration.[11] Although physiologically unique and designated as a protease inhibitor, SLPI has the structural characteristics of a WFDC domain. Chromosome 20q13 was recently recognized as the WFDC locus, containing the genes encoding 14 WFDC-type protease inhibitors.[12] The WFDC-encoded proteins are thought to play roles in innate immunity and in regulating endogenous kallikreins, and are expressed predominantly in the epididymis, testis, and trachea. More recently, the WFDC locus was reported to have undergone rapid divergence in the primate lineage.[13] WFDC-type protease inhibitors also differ considerably between human and mouse. For example, elafin, another airway WFDC-type protease inhibitor, has no ortholog in the mouse. To search for new WFDC-type protease inhibitors, we cloned the mouse *SWAM1* and *SWAM2* genes and showed that both gene products are antibacterial.[14] In

[1]To whom correspondence should be addressed.
E-mail: toshinkw@idac.tohoku.ac.jp

doi: 10.1111/j.1349-7006.2008.00772.x

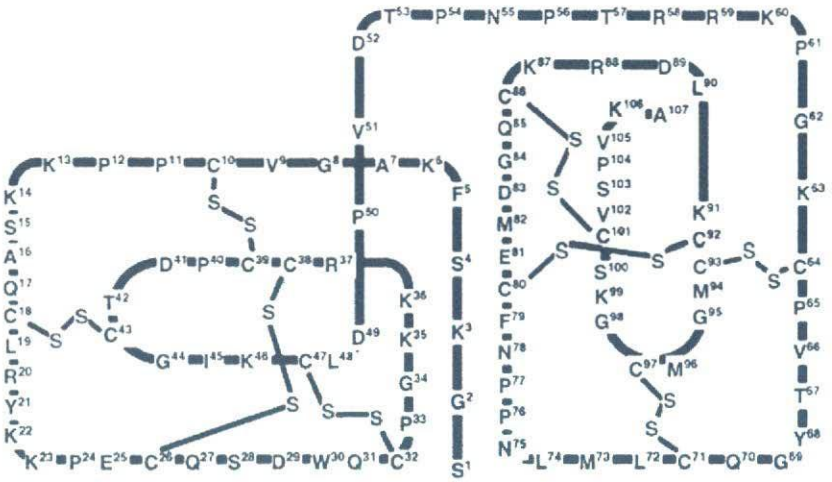

Fig. 1. Schematic representation of the polypeptide chain arrangement of human secretory leukocyte peptidase inhibitor (SLPI). SLPI consists of 107 amino acids with a boomerang-shaped structure composed of two topologically superimposable domains: an N-terminal domain consisting of Ser^{1}–Pro^{54} and a C-terminal domain consisting of Asn^{55}–Ala^{107}. Four disulfide bridges are present in each domain (indicated by thin lines).

summary, SLPI is secreted in the lining fluid of the airways, and works as an antiprotease and has unknown innate immune functions.

Complicated function of SLPI

Protease inhibitor. SLPI was originally discovered as a protein with antiprotease activity, and this is its major function. Although it consists of two similar domains, the antiprotease active site of SLPI is Leu^{72}-Met^{73} in a loop (residues 67–74) on the C-terminal domain.[2] SLPI inhibits elastase, cathepsin G, trypsin, chymotrypsin, chymase, and tryptase. However, its physiological target is neutrophil elastase, because SLPI accounts for approximately 90% of all elastase inhibitors in human bronchial secretions, and it has high affinity for neutrophil elastase.[1] Experiments in *SLPI* knockout mice clarified the balance of SLPI and elastase in a model of wound healing. Ashcroft *et al.* reported high elastase activity, large amounts of active transforming growth factor (TGF)-β in the wound, and impaired healing in *SLPI* knockout mice.[15] Zhu *et al.* analyzed this mechanism further and reported that SLPI protects proepithelin (also called progranulin) from cleavage by neutrophil elastase.[16] In *SLPI* knockout mice, proepithelin is cleaved into epithelins, which recruit more neutrophils and suppress epithelial cell growth. Several recent reports have described SLPI as being inactivated by proteolytic cleavage by cathepsins and bacterial proteases. At sites of inflammation, the balance between the processes involved in augmenting the innate immune reaction and tissue repair and regeneration is controlled by the relative amounts of neutrophil elastase and its inhibitor SLPI (Fig. 2; Table 2). Considering normal wound healing in individuals with a deficiency in α-1-antitrypsin, another antiprotease for neutrophil elastase, the function of SLPI in tissue repair and maintenance appears to be highly specialized.

Table 1. Relative expression of secretory leukocyte peptidase inhibitor (SLPI) mRNA in human tissue

Organ	Relative expression (%)
Trachea	100
Bronchus	85
Oral mucosa	51
Salivary gland	46
Pharyngeal mucosa	29
Esophagus	20
Lung	11
Vagina	7
Mammary gland	4
Tonsil	4
Adipose tissue	3
Bone marrow	2
Liver	2
Prostata grand	1
Colon cecum	1
Thyroid gland	1
Testis	1
Kidney medulla	1
Adrenal cortex	1
Skeletal muscle	1
Kidney cortex	0
Ovary	0
Lymph node	0
Spleen	0

Adopted from the microarray data from GSE3526 that analyzed representative normal tissue from 10 postmortem donors using Affymetrix U133 plus 2.0. The average value of the expression of the SLPI mRNA transcripts from three to five donors were sorted and shown as relative expression (%).

Antimicrobial and anti-human immunodeficiency virus (HIV) capacity. Hiemstra *et al.* discovered an SLPI-like peptide from equine neutrophils with antimicrobial capacity, although they reported that the antimicrobial activity of SLPI was less than those of lysozyme or defensins.[17] They also found that the residues with antimicrobial activity were located in the N-terminal domain, in contrast to the antiprotease activity. Although the precise mechanism underlying the antimicrobial capacity of SLPI remains unclear, the possible involvement of the cationic nature of the WFDC domains is suggested by previous findings that eNap-2, a cationic polypeptide with features characteristic of the WFDC family, displays antibacterial activity.[18,19]

Ma *et al.* reported that SLPI prevents HIV transmission. They demonstrated that SLPI binds to the membrane of human macrophages through a phospholipid binding protein, annexin II, which is a cellular cofactor that acts as a phosphatidylserine-binding moiety.[20] Annexin II supports macrophage HIV-1 infection and SLPI disrupts the interaction (Fig. 2). These antimicrobial and anti-HIV capacities of SLPI may be effective because of its high concentration in the airway lining fluid.

Immunomodulatory and anti-inflammatory functions. In an early clinical study of the administration of recombinant SLPI to patients with cystic fibrosis, McElvaney *et al.* reported that there were reductions in interleukin (IL)-8 and neutrophil elastase in the bronchoalveolar lavage fluid from these patients after

doi: 10.1111/j.1349-7006.2008.00772.x

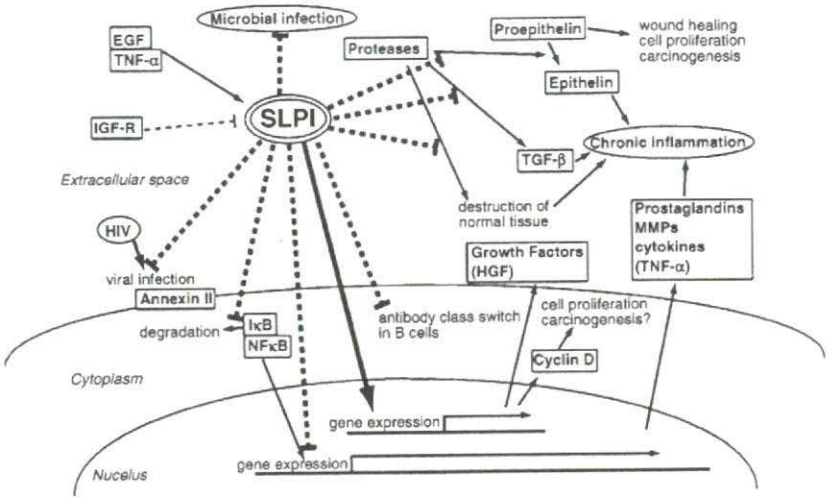

Fig. 2. A schema of the various reported biological functions of secretory leukocyte peptidase inhibitor (SLPI). A major physiological role of SLPI is thought to be antineutrophil elastase protection at sites of inflammation. In addition, recent studies have revealed that SLPI has several biological properties, some of which are independent of its protease inhibitor activity.

Table 2. Biological functions of secretory leukocyte peptidase inhibitor (SLPI)

Effect on pathway	Target	Mechanism of regulation
Control of inflammation		
Suppression of epithelin[16]	Epithelin	Dependent of antiprotease activity
Decrease TNF-α, MCP-1, IL-6 expression[25]	TNF-α	Dependent of antiprotease activity
	MCP-1	
	IL-6	
Increase HGF expression[29]	HGF	Dependent of antiprotease activity
Suppression of PGE2, MMP1, MMP9[27]	PGE_2	Independent of antiprotease activity
	MMP1	
	MMP9	
Decrease TGF-β activity[15,30]	TGF-β	Regulating gene expression?
		Dependent of antiprotease activity?
Increase TGF-β, IL-10[26]	TGF-β	Unknown mechanism
	IL-10	
Suppression of class switch[24]	AID?	Inhibition of AID induction
Suppression of NF-κB activity[8,23]	IκBβ	Inhibition of IκB-β degradation?
	NF-κB	Inhibition of NF-κB and DNA binding?
Cell proliferation		
Increase cyclin D expression[30]	Cyclin D	Unknown mechanism
Anti-infection		
Anti-HIV-infection[20]	Annexin II	Binding to annexin II
Antimicrobial infection[17]	Unknown	Unknown
		Independent of antiprotease activity

AID, activation-induced cytidine deaminase; HGF, hepatocyte growth factor; HIV, human immunodeficiency virus; IL, interleukin; MCP, monocyte chemoattractant protein-1; MMP, matrix metalloprotease; NF, nuclear factor; PGE, prostaglandin E; TGF, transforming growth factor; TNF, tumor necrosis factor.

inhalation of aerosolized SLPI.[21] Subsequent studies showed that SLPI exerts its immunomodulatory effects through attenuation of nuclear factor (NF)-κB. We constructed *SLPI* knockout mice, and examined the changes in immune-related factors after lipopolysaccharide (LPS) administration.[22] In $SLPI^{-/-}$ mice after LPS administration, the survival rate was lower than that of wild-type (WT) controls, and high levels of serum IL-6, but not IL-1β, tumor necrosis factor (TNF)-α, or NO_2^- were noted. High mobilty group B1 (HMGB1) in macrophages was increased in $SLPI^{-/-}$ mice. In $SLPI^{-/-}$ mice, IκB-β was suppressed after LPS administration. In contrast, the DNA-binding activities of NF-κB and CCAAT/enhancer binding protein (C/EPP)-β were stronger in $SLPI^{-/-}$ macrophages.[22] We also reported that splenic B cells from $SLPI^{-/-}$ mice had higher proliferation rates and produced higher levels of Ig M. One of the mechanisms for the regulation of NF-κB activation by SLPI was assumed to be that SLPI elevates the protein, not mRNA, level of IκB-β, a NF-κB inhibitor.[23] Recently, Taggart *et al.* reported that on incubation with the U937 monocytic cell line or peripheral blood monocytes, SLPI enters the cells and is rapidly localized to the cytoplasm and nucleus where it affects NF-κB activation by direct binding to NF-κB sites in a site-specific manner[8] (Fig. 2). This was confirmed recently by Xu *et al.* who showed that SLPI from tonsillar epithelial cells restrained class switching by inhibiting activation-induced cytidine deaminase (AID) induction in B cells, and again they found SLPI in the nucleus and cytoplasm.[24]

Control of inflammation and tissue repair. There have been many reports of the attenuation of inflammation by SLPI. It has been reported that the production of TNF-α, monocyte chemoattractant protein-1 (MCP-1), and IL-6 in macrophages is downregulated,[25]

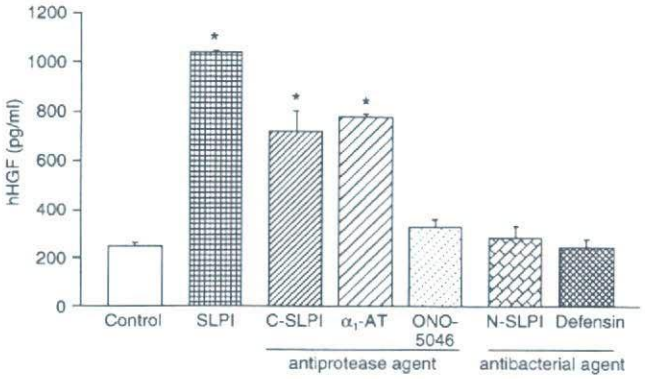

Fig. 3. Effects of secretory leukocyte peptidase inhibitor (SLPI) on hepatocyte growth factor (HGF) production by human lung fibroblasts.[29] Human lung fibroblast CCD-11Lu cells were cultured for 16 h under the following conditions: control, no addition; SLPI, 10 μM full-length SLPI; C-SLPI, 10 μM C-terminal domain of SLPI; α1-AT, 50 μg/mL human α1-antitrypsin; ONO-5046, 10 μM synthetic neutrophil elastase inhibitor; N-SLPI, 10 μM N-terminal domain of SLPI; defensin, 2.5 μg/mL human neutrophil peptides (HNP)-1. The concentrations of human HGF (hHGF) in the culture medium were determined by enzyme-linked immunosorbent assay. The results are shown as the mean ± SEM ($n = 3$ per data point). Asterisks indicate significant differences at the 95% confidence level compared with control cells.

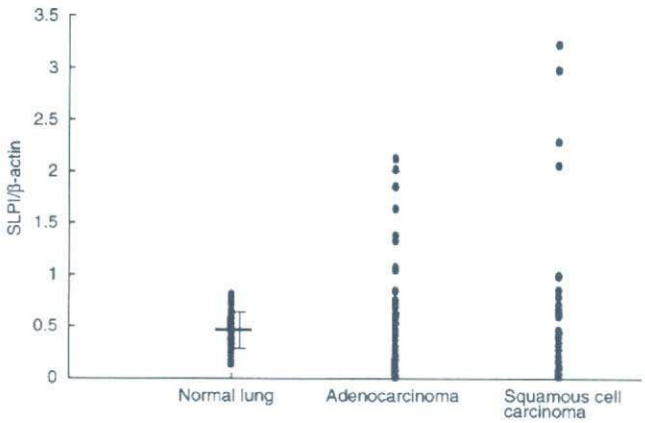

Fig. 4. Comparison of secretory leukocyte peptidase inhibitor (SLPI) expression in normal tissue, lung adenocarcinoma, and squamous cell carcinoma. The data were extracted from the NCBI GEO DataSets GSE1643 (normal lung, 40 samples,[5] and GSE3141 lung adenocarcinoma, 58 samples; squamous cell carcinoma, 53 samples).[34] The probe ID in the Affymetrix platforms were 2030211_at (SLPI) and AFFX-HSAC07/X00351-5_at (β-actin). The relative expression ratios of SLPI to β-actin were evaluated.

whereas the expression of the anti-inflammatory cytokines IL-10 and TGF-β is upregulated.[26] Ashcroft *et al.* reported high TGF-β activity in SLPI-deficient mice,[15] although some inconsistencies, especially about TGF-β and TNF-α, were noted due to the experimental systems used (Table 2). SLPI decreased the production of cyclooxygenase (COX)-2, PGE_2, matrix metalloprotease (MMP)-1, and MMP-9 with the result of suppressed tissue injury.[27] Mouse SLPI was purified from mouse fibroblasts as a scatter factor- or hepatocyte growth factor (HGF)-inducing factor,[28] and so we examined HGF induction by SLPI. Our results indicated that SLPI induced HGF from human fibroblasts in a time- and dose-dependent manner.[29] Moreover, HGF was induced by the C-terminal domain of SLPI, but not by the N-terminal half of SLPI or by defensin (Fig. 3). Interestingly, α-1-antitrypsin also induced HGF, but not ONO-5046, an elastase inhibitor. Zhang *et al.* reported that *cyclin D1* gene expression was elevated when SLPI was expressed.[30] Cyclin D1 may be associated with cell proliferation during tissue repair.[30] Therefore, SLPI acts as a multifunctional defense factor: as an antiprotease to promote wound healing, by controlling pro-inflammatory factors by suppression of the action of NF-κB, suppression of COX-2 and PGE_2, and by induction of HGF, a tissue-regenerating factor, from mesenchymal cells (Fig. 2).

Secretory leukocyte peptidase inhibitor and cancer

Overexpression and downregulation of SLPI. Based on the tissue distribution of SLPI expression, neoplasms of the respiratory, digestive, and reproductive tracts should express SLPI transcripts and protein. Bouchard *et al.* reported in their review[6] that SLPI expression is highly upregulated in pancreatic, papillary thyroid, uterine cervix, endometrial, and ovarian cancer; by contrast, SLPI is underexpressed in nasopharyngeal carcinoma, bladder tumors, and some breast carcinoma, although overexpression of this protein correlates with more-invasive forms of breast carcinoma. Although the underlying mechanisms have not been fully elucidated, Devoogdt *et al.* suggested that, at least in female cancers, the amplification of chromosome 20q (20q12 to q13.2) encoding the *SLPI* gene may result in increased SLPI expression.[31,32]

Secretory leukocyte peptidase inhibitor in lung cancer. Immunostaining with anti-SLPI antibody indicates that lung cancer tissue contains SLPI protein. Ameshima *et al.* reported that the SLPI concentration in serum is higher in patients with lung cancer than in healthy controls (71.5 ± 2.4 vs 50.5 ± 1.5 ng/mL, $P < 0.005$), higher in advanced cases of NSCLC (stages III and IV), and decreased after effective treatment,[33] indicating that the serum SLPI level reflects the tumor volume. However, in the gene-expression profiling data for lung cancer (NCBI GEO DataSet GSE3141), the levels of SLPI transcripts in lung adenocarcinoma or squamous cell carcinoma are not always upregulated.[34] The average SLPI to β-actin expression ratio in the normal lung is 0.47 ± 0.17 (mean ± SD)[5] whereas 24 and 23% of adenocarcinoma and squamous cell carcinoma samples, respectively, expressed more than the range of SD in normal lung samples, and 43 and 40%, respectively, expressed less than the SD range (Fig. 4). Several factors such as inflammatory cytokines and steroid hormones have been reported to affect *SLPI* gene expression.[31] The scattering result of SLPI transcripts in lung tumors may be due to the various clinical settings of the tumor samples.

As SLPI is a secretory protein and is expressed at levels similar to those of highly expressed proteins, such as surfactants, the promoter regions of the *SLPI* gene can be utilized for lung cancer-specific expression of transgenes by intratumoral injection. We applied this idea in a preclinical experimental system of a replication-competent adenovirus vector for NSCLC.[35] A large xenograft (approximately 600 mm^3) of H358 cells in nude mice was effectively reduced in size with a single intratumoral dose of combined AdSLPI.E1AdB (adenovirus aimed for high *E1A* gene expression under the SLPI promoter in lung cancer) and AdCMV.NK4 (NK4; N-terminal truncated HGF that antagonizes HGF, vascular endothelial growth factor (VEGF), and fibroblast growth factor (FGF)[36]) indicating the advantages of utilizing the promoter of the highly expressed *SLPI* gene.

Upregulation of SLPI in the gene expression profiles under tumorigenic conditions: Microarray analysis and SLPI transfection. As SLPI functions physiologically as an anti-inflammatory agent and plays a role in tissue regeneration, the *SLPI* gene is often amplified under conditions related to tumorigenesis. When phorbol-12-myristate-13-acetate (TPA) was applied to mouse skin to produce chemical carcinogenesis, the SLPI expression in

doi: 10.1111/j.1349-7006.2008.00772.x

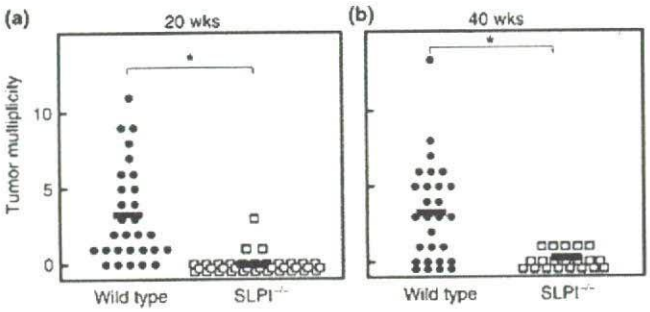

Fig. 5. Decreased susceptibility to urethane-induced lung tumors in secretory leukocyte peptidase inhibitor (SLPI)-deficient mice. Wild-type or *SLPI*$^{-/-}$ mice were injected intraperitoneally with urethane (1 mg/g bodyweight). The animals were killed (a) 20 or (b) 40 weeks later, and the number of macroscopic external pulmonary nodules was counted. Each bar represents the mean of the group: (a) wild-type, $n = 29$ mice; *SLPI*$^{-/-}$, $n = 36$ mice; (b) wild-type, $n = 28$ mice; *SLPI*$^{-/-}$, $n = 19$ mice. Asterisks indicate significant differences at the 95% confidence level between wild-type and *SLPI*$^{-/-}$ mice.

the treated skin was upregulated 6 h after TPA induction.[37] When low-malignant Lewis lung carcinoma 3LL-S cells were inoculated subcutaneously, and high-malignant 3LL-S-sc cells were isolated from the subcutaneous tumor, the subtraction procedure used to identify genes modulated during the subcutaneous growth of 3LL-S cells identified mouse SLPI.[38] Transfection of the mouse or human *SLPI* gene into 3LL-S cells enhanced tumor growth, but tumor formation by these transfectants was not related to *in vitro* cell proliferation. SLPI, HSP-70, and CXCL-1 were identified among 106 genes expressed differentially >2.5-fold between poorly metastatic and highly metastatic variants of human breast cancer cell lines, GI101A and GILM2, respectively.[39] Viatour *et al.* reported that glycogen synthase kinase (GSK) 3-mediated B cell lymphoma (BCL)-3 phosphorylation modulates its degradation and upregulates the expression of SLPI, CXCL-1, interferon activated gene (IFI)205, and cytochrome P4SO 1B1 (CYP1B1).[40]

In addition, *SLPI* was identified as a potential regulatory gene in the microarray expression profile at markedly higher levels (>2 log difference) in non-metastatic 3LL M-27 lung carcinoma cells compared with liver-metastatic 3LL H-59 lung carcinoma cells.[41] Wang *et al.* transfected the *SLPI* gene into H-59, and showed that SLPI from transfected H-59 cells suppressed TNF-α production from a macrophage cell line *in vitro* by regulation of NF-κB, and inhibited TNF-α induction as well as E-selectin in response to infiltrating tumor cells, and ultimately suppressed experimental liver metastasis *in vivo*.[41] Interestingly, Devoogdt *et al.* reported that the tumor-promoting effect of TNF-α involves the induction of SLPI.[42] They used cancer cell lines derived from subcutaneous nodules of 3LL-S cells in WT mice (3LL-S-sc WT) and *TNF-α* knockout mice (3LL-S-sc KO). Although the tumor growth of 3LL-S-sc WT cells was higher than that of 3LL-S-sc KO cells, SLPI was expressed in larger amounts in 3LL-S-sc WT cells[42] suggesting that endogenous TNF-α contributed to SLPI protein production at the tumor site. Interestingly, 3LL-S cells transfected with SLPI small interfering RNA (siRNA) showed no tumor formation in WT mice.[42]

Finally, Sugino *et al.* reported that SLPI promotes blood-borne metastasis via an invasion-independent pathway.[43] They transfected the *SLPI* gene into a poorly metastatic clone of the MCH66 mouse mammary tumor cell line. Although SLPI-transfected cells showed a less-invasive nature in a Matrigel assay, *in vivo* inoculation of SLPI-transfected cells into the mammary fat pads resulted in greater lung and lymph node metastasis. Histological examination revealed that SLPI-transfected tumors formed a well-developed CD31-positive sinusoidal vasculature surrounding the tumor nests, where tumor cells are supposed to enter the circulation without vascular invasion.[43] In fact, these tumors showed intravascular growth and the formation of metastatic nodules in the lung. Based on these results, the authors proposed the functional role of SLPI in the invasion-independent metastatic potential of cancer cells.[43]

In summary, how the SLPI expression of cancer cells affects metastatic potential remains to be fully defined; specifically, the higher SLPI expression in higher-metastatic breast cancer cell lines[41,43] and, in contrast, the higher SLPI expression in non-metastatic lung cancer cells.[39] The discordance among previous reports may depend on the experimental conditions used, such as cell line.

Carcinogenesis is suppressed in the *SLPI* knockout mouse

Urethane carcinogenesis. To investigate whether SLPI induces carcinogenesis or restrains the growth of cancer tissue, we induced chemical carcinogenesis using urethane. When urethane was administered intraperitoneally to WT mice at a dose of 1 mg/g bodyweight, urethane-induced tumors in the lung were visible at 20 or 40 weeks. The induced tumors were lung adenocarcinoma-like histologically, and the tumor cells showed strong staining with anti-SLPI antibody. When we administered urethane to *SLPI* knockout mice, negligible tumor formation was detected at 20 or 40 weeks (Fig. 5). We confirmed that urethane-metabolizing CYP2e1 is expressed in both WT and *SLPI*$^{-/-}$ mice.

Working hypothesis and further analyses. The functions of SLPI include: (i) its action as an extracellular protease inhibitor; (ii) penetration of the cytoplasm and nucleus in monocytes and macrophages to elicit anti-inflammatory effects through suppression of NF-κB function; and (iii) the induction of HGF from fibroblasts (Fig. 2). We have not succeeded in analyzing completely the suppression of urethane-induced tumor formation in *SLPI*$^{-/-}$ mice. Even without SLPI function, some microseeds of tumor cells are formed, as determined by the low number of tumors in *SLPI*$^{-/-}$ mice at 20 or 40 weeks. The effects of SLPI in the tumor cells and in the surrounding stromal cells must be considered separately. When both tumor cells and environmental stromal cells contain SLPI, urethane-induced tumors are formed. Conversely, when neither tumor cells nor environmental stromal cells contain SLPI, tumor formation is suppressed. In this context, the observation that 3LL-S cells transfected with SLPI siRNA did not form tumors, as reported by Devoogdt *et al.*,[42] indicated that the SLPI in tumor cells, but not that in the environmental stromal cells, is essential for tumor formation. Whether 3LL cells transfected with the *SLPI* gene inoculated into *SLPI*$^{-/-}$ mice (i.e. tumor cells are SLPI^{+} and environmental stromal cells are SLPI^{-}) can form tumors is another essential question. In this regard, 3LL cells inoculated into *SLPI*$^{-/-}$ mice grew in the same manner as in WT mice, at least with subcutaneous inoculation (unpublished observation, Zaini and Nukiwa, 2007).

Gene expression in the lungs was examined in microarray analyses of WT and *SLPI*$^{-/-}$ mice, and interesting genes upregulated in the lungs of *SLPI*$^{-/-}$ mice are currently under investigation. SLPI binds to a number of proteins, such as proepithelin and annexin II. In a yeast two-hybrid assay, we detected 18 partner candidate proteins, including both proepithelin and annexin II.[44] The direct protein–protein interaction of SLPI would be another route for investigating SLPI function in tumorigenesis.

Finally, we noticed that some lung adenocarcinoma cell lines with epidermal growth factor receptor (EGFR) kinase-activating mutations express and secrete large amounts of SLPI. The production of SLPI is suppressed by gefitinib, an inhibitor of EGFR

kinase, but the effect is not complete. The role of SLPI in the EGFR signaling pathway in SLPI-induced tumorigenesis should be examined in future studies.

Perspectives

Although located at a very unstable locus in chromosome 20q, SLPI is conserved in mammals, and abundant SLPI is produced in the respiratory and reproductive tracts. These observations are the background to the unique function of SLPI in cell physiology. In studies to clarify the function of SLPI, we noticed an unexpected phenotype in *SLPI*$^{-/-}$ mice: suppression of urethane-induced carcinogenesis in the lung. There is accumulating evidence that a paucity of SLPI in cancer cells suppresses tumor formation. The control of elastase activity in the treatment of cancer is not generally accepted. However, Sato *et al.* used ONO-5046, a synthetic elastase inhibitor, to suppress the growth of EBC-1 lung cancer.[45] However, SLPI has the opposite effect. SLPI expression is upregulated in tumor formation, and the absence of SLPI production does not promote tumor formation. Because urethane-induced carcinogenesis in the lung is suppressed in *SLPI*$^{-/-}$ mouse, further analysis of SLPI function in relation to the tumor-forming capacity may lead to the development of a novel treatment modality.

Acknowledgments

We thank Dr Takashi Tsuruo for encouragement regarding this review. The authors also thank our colleagues Drs Tatsuya Abe, Yuriko Mori, Akira Nakamura, Toshiyuki Takai, Koichi Hagiwara, and Daizo Koinuma for their efforts in the construction and analysis of SLPI knockout mice.

References

1 Abe T, Kobayashi N, Yoshimura K *et al.* Expression of the secretory leukoprotease inhibitor gene in epithelial cells. *J Clin Invest* 1991; **87**: 2207–15.
2 Weldon S, McGarry N, Taggart CC, McElvaney NG. The role of secretory leucoprotease inhibitor in the resolution of inflammatory responses. *Biochem Soc Trans* 2007; **35**: 273–6.
3 Doumas S, Kolokotronis A, Stefanopoulos P. Anti-inflammatory and antimicrobial roles of secretory leukocyte protease inhibitor. *Infect Immun* 2005; **73**: 1271–4.
4 Jin FY, Nathan C, Radzioch D, Ding A. Secretory leukocyte protease inhibitor: a macrophage product induced by and antagonistic to bacterial lipopolysaccharide. *Cell* 1997; **88**: 417–26.
5 Gruber MP, Coldren CD, Woolum MD *et al.* Human lung project: evaluating variance of gene expression in the human lung. *Am J Respir Cell Mol Biol* 2006; **35**: 65–71.
6 Bouchard D, Morisset D, Bourbonnais Y, Tremblay GM. Proteins with whey-acidic-protein motifs and cancer. *Lancet Oncol* 2006; **7**: 167–74.
7 Iacobuzio-Donahue CA, Ashfaq R, Maitra A *et al.* Highly expressed genes in pancreatic ductal adenocarcinomas: a comprehensive characterization and comparison of the transcription profiles obtained from three major technologies. *Cancer Res* 2003; **63**: 8614–22.
8 Taggart CC, Cryan SA, Weldon S *et al.* Secretory leucoprotease inhibitor binds to NF-κB binding sites in monocytes and inhibits p65 binding. *J Exp Med* 2005; **202**: 1659–68.
9 Abe T, Tominaga Y, Kikuchi T *et al.* Bacterial pneumonia causes augmented expression of the secretory leukoprotease inhibitor gene in the murine lung. *Am J Respir Crit Care Med* 1997; **156**: 1235–40.
10 Kikuchi T, Abe T, Satoh K *et al.* Cis-acting region associated with lung cell-specific expression of the secretory leukoprotease inhibitor gene. *Am J Respir Cell Mol Biol* 1997; **17**: 361–7.
11 Kikuchi T, Abe T, Hoshi S *et al.* Structure of the murine secretory leukoprotease inhibitor (Slpi) gene and chromosomal localization of the human and murine SLPI genes. *Am J Respir Cell Mol Biol* 1998; **19**: 875–80.
12 Clauss A, Lilja H, Lundwall A. A locus on human chromosome 20 contains several genes expressing protease inhibitor domains with homology to whey acidic protein. *Biochem J* 2002; **368**: 233–42.
13 Hurle B, Swanson W, Green ED. Comparative sequence analyses reveal rapid and divergent evolutionary changes of the WFDC locus in the primate lineage. *Genome Res* 2007; **17**: 276–86.
14 Hagiwara K, Kikuchi T, Endo Y *et al.* Mouse SWAM1 and SWAM2 are antibacterial proteins composed of a single whey acidic protein motif. *J Immunol* 2003; **170**: 1973–9.
15 Ashcroft GS, Lei K, Jin W *et al.* Secretory leukocyte protease inhibitor mediates non-redundant functions necessary for normal wound healing. *Nat Med* 2000; **6**: 1147–53.
16 Zhu J, Nathan C, Jin W *et al.* Conversion of proepithelin to epithelins: roles of SLPI and elastase in host defense and wound repair. *Cell* 2002; **111**: 867–78.
17 Hiemstra PS, Maassen RJ, Stolk J, Heinzel-Wieland R, Steffens GJ, Dijkman JH. Antibacterial activity of antileukoprotease. *Infect Immun* 1996; **64**: 4520–4.
18 Couto MA, Harwig SS, Cullor JS, Hughes JP, Lehrer RI. eNAP-2, a novel cysteine-rich bactericidal peptide from equine leukocytes. *Infect Immun* 1992; **60**: 5042–7.
19 Couto MA, Harwig SS, Lehrer RI. Selective inhibition of microbial serine proteases by eNAP-2, an antimicrobial peptide from equine neutrophils. *Infect Immun* 1993; **61**: 2991–4.
20 Ma G, Greenwell-Wild T, Lei K *et al.* Secretory leukocyte protease inhibitor binds to annexin II, a cofactor for macrophage HIV-1 infection. *J Exp Med* 2004; **200**: 1337–46.
21 McElvaney NG, Nakamura H, Birrer P *et al.* Modulation of airway inflammation in cystic fibrosis. *In vivo* suppression of interleukin-8 levels on the respiratory epithelial surface by aerosolization of recombinant secretory leukoprotease inhibitor. *J Clin Invest* 1992; **90**: 1296–301.
22 Nakamura A, Mori Y, Hagiwara K *et al.* Increased susceptibility to LPS-induced endotoxin shock in secretory leukoprotease inhibitor (SLPI)-deficient mice. *J Exp Med* 2003; **197**: 669–74.
23 Lentsch AB, Jordan JA, Czermak BJ *et al.* Inhibition of NF-κB activation and augmentation of IκBβ by secretory leukocyte protease inhibitor during lung inflammation. *Am J Pathol* 1999; **154**: 239–47.
24 Xu W, He B, Chiu A *et al.* Epithelial cells trigger frontline immunoglobulin class switching through a pathway regulated by the inhibitor SLPI. *Nat Immunol* 2007; **8**: 294–303.
25 Greene CM, McElvaney NG, O'Neill SJ, Taggart CC. Secretory leucoprotease inhibitor impairs Toll-like receptor 2- and 4-mediated responses in monocytic cells. *Infect Immun* 2004; **72**: 3684–7.
26 Sano C, Shimizu T, Sato K, Kawauchi H, Tomioka H. Effects of secretory leucocyte protease inhibitor on the production of the anti-inflammatory cytokines, IL-10 and transforming growth factor-beta (TGF-β), by lipopolysaccharide-stimulated macrophages. *Clin Exp Immunol* 2000; **121**: 77–85.
27 Zhang Y, DeWitt DL, McNeely TB, Wahl SM, Wahl LM. Secretory leukocyte protease inhibitor suppresses the production of monocyte prostaglandin H synthase-2, prostaglandin E2, and matrix metalloproteinases. *J Clin Invest* 1997; **99**: 894–900.
28 Rosen EM, Knesel J, Goldberg ID *et al.* Scatter factor modulates the metastatic phenotype of the EMT6 mouse mammary tumor. *Int J Cancer* 1994; **57**: 706–14.
29 Kikuchi T, Abe T, Yaekashiwa M *et al.* Secretory leukoprotease inhibitor augments hepatocyte growth factor production in human lung fibroblasts. *Am J Respir Cell Mol Biol* 2000; **23**: 364–70.
30 Zhang D, Simmen RC, Michel FJ, Zhao G, Vale-Cruz D, Simmen FA. Secretory leukocyte protease inhibitor mediates proliferation of human endometrial epithelial cells by positive and negative regulation of growth-associated genes. *J Biol Chem* 2002; **277**: 29 999–30 009.
31 Devoogdt N, Revets H, Ghassabeh GH, De Baetselier P. Secretory leukocyte protease inhibitor in cancer development. *Ann NY Acad Sci* 2004; **1028**: 380–9.
32 Israeli O, Goldring-Aviram A, Rienstein S *et al.* *In silico* chromosomal clustering of genes displaying altered expression patterns in ovarian cancer. *Cancer Genet Cytogenet* 2005; **160**: 35–42.
33 Ameshima S, Ishizaki T, Demura Y, Imamura Y, Miyamori I, Mitsuhashi H. Increased secretory leukoprotease inhibitor in patients with nonsmall cell lung carcinoma. *Cancer* 2000; **89**: 1448–56.
34 Bild AH, Yao G, Chang JT *et al.* Oncogenic pathway signatures in human cancers as a guide to targeted therapies. *Nature* 2006; **439**: 353–7.
35 Maemondo M, Saijo Y, Narumi K *et al.* Gene therapy with secretory leukoprotease inhibitor promoter-controlled replication-competent adenovirus for non-small cell lung cancer. *Cancer Res* 2004; **64**: 4611–20.
36 Kuba K, Matsumoto K, Date K, Shimura H, Tanaka M, Nakamura T. HGF/NK4, a four-kringle antagonist of hepatocyte growth factor, is an angiogenesis inhibitor that suppresses tumor growth and metastasis in mice. *Cancer Res* 2000; **60**: 6737–43.

doi: 10.1111/j.1349-7006.2008.00772.x

37 Schlingemann J, Hess J, Wrobel G *et al.* Profile of gene expression induced by the tumour promotor TPA in murine epithelial cells. *Int J Cancer* 2003; **104**: 699–708.
38 Devoogdt N, Hassanzadeh Ghassabeh G, Zhang J, Brys L, De Baetselier P, Revets H. Secretory leukocyte protease inhibitor promotes the tumorigenic and metastatic potential of cancer cells. *Proc Natl Acad Sci USA* 2003; **100**: 5778–82.
39 Kluger HM, Chelouche Lev D, Kluger Y *et al.* Using a xenograft model of human breast cancer metastasis to find genes associated with clinically aggressive disease. *Cancer Res* 2005; **65**: 5578–87.
40 Viatour P, Dejardin E, Warnier M *et al.* GSK3-mediated BCL-3 phosphorylation modulates its degradation and its oncogenicity. *Mol Cell* 2004; **16**: 35–45.
41 Wang N, Thuraisingam T, Fallavollita L, Ding A, Radzioch D, Brodt P. The secretory leukocyte protease inhibitor is a type 1 insulin-like growth factor receptor-regulated protein that protects against liver metastasis by attenuating the host proinflammatory response. *Cancer Res* 2006; **66**: 3062–70.
42 Devoogdt N, Revets H, Kindt A, Liu YQ, De Baetselier P, Ghassabeh GH. The tumor-promoting effect of TNF-α involves the induction of secretory leukocyte protease inhibitor. *J Immunol* 2006; **177**: 8046–52.
43 Sugino T, Yamaguchi T, Ogura G *et al.* The secretory leukocyte protease inhibitor (SLPI) suppresses cancer cell invasion but promotes blood-borne metastasis via an invasion-independent pathway. *J Pathol* 2007; **212**: 152–60.
44 Nukiwa T, Suzuki T. Effect of tobacco smoke in the intracellular trafficking of type II alveolar epithelial cells. *Smoking Res Foundation Annu Res Report* 2004; **10**: 409–14.
45 Sato T, Takahashi S, Mizumoto T *et al.* Neutrophil elastase and cancer. *Surg Oncol* 2006; **15**: 217–22.

Suppression of surfactant protein A by an epidermal growth factor receptor tyrosine kinase inhibitor exacerbates lung inflammation

Akira Inoue,[1] Hong Xin,[2] Takuji Suzuki,[1] Masahiko Kanehira,[1,2] Yoshio Kuroki,[3] Tatsuro Fukuhara,[1] Toshiaki Kikuchi,[1] Makoto Maemondo,[4] Toshihiro Nukiwa[1] and Yasuo Saijo[2,5,6]

[1]Department of Respiratory Oncology and Molecular Medicine, Institute of Development, Aging and Cancer, Tohoku University, Seiryomachi 4-1 Aobaku, Sendai 980-8575; [2]Department of Molecular Medicine, Tohoku University Graduate School of Medicine, Seiryomachi 2-1 Aobaku, Sendai 980-8575; [3]Department of Biochemistry, Sapporo Medical University School of Medicine, Sapporo 060-8556; [4]Miyagi Cancer Center Hospital, Natori 981-1293; [5]Department of Medical Oncology, Hirosaki University Graduate School of Medicine, Zaifucho 5, Hirosaki, 036-8562, Japan

(Received December 22, 2007/Revised April 14, 2008/Accepted April 14, 2008/Online publication July 29, 2008)

Interstitial lung disease (ILD) is reported as a serious adverse event in lung cancer patients treated with gefitinib, an epidermal growth factor receptor tyrosine kinase inhibitor (EGFR-TKI). However, the mechanisms of ILD associated with gefitinib remain unknown. To address the molecular mechanisms of ILD-associated gefitinib, we determined the effect of gefitinib treatment on surfactant protein expression *in vitro* and *in vivo*. Gefitinib treatment suppressed surfactant protein (SP)-A expression in H441 human lung adenocarcinoma cells expressing SP-A, -B, -C and -D by inhibiting epidermal growth factor signal. Next, gefitinib (200 mg/kg) was given p.o. to the mice daily for 1 week. Daily administration of gefitinib gradually reduced SP-A level in the bronchoalveolar lavage fluid. When lipopolysaccharide (LPS) was instilled intratracheally to the mice pretreated with gefitinib for 1 week, lung inflammation by LPS was exacerbated and prolonged. This exacerbation of lung inflammation was rescued by intranasal administration of SP-A. These results demonstrated that pretreatment with gefitinib exacerbated LPS-induced lung inflammation by reducing SP-A expression in the lung. This study suggests that epidermal growth factor receptor tyrosine kinase inhibitor may reduce SP-A expression in the lungs of lung cancer patients and thus patients treated with epidermal growth factor receptor tyrosine kinase inhibitor may be susceptible to pathogens. (*Cancer Sci* 2008; 99: 1679–1684)

Gefitinib is an epidermal growth factor receptor (EGFR) tyrosine kinase inhibitor (TKI) that has antitumor activity in patients with advanced non-small cell lung cancer (NSCLC). Two large phase II trials for previously treated advanced NSCLC revealed that gefitinib monotherapy was effective, with response rates of 18.4% and 12%.[1,2] Higher response rates were achieved in Japanese, non-smoking and adenocarcinoma patients,[3] and subsequent reports revealed that some somatic mutations of the EGFR gene, frequently observed in these patients, are strongly correlated with sensitivity to gefitinib.[4,5] The most common adverse effects associated with gefitinib are skin rash and diarrhea; these were generally mild in the phase II clinical trials and have been confirmed in extensive clinical practice.[1,2]

Interstitial lung disease (ILD) was reported as a serious adverse event associated with gefitinib after its approval in Japan.[6–8] Retrospective analysis revealed that, in Japan, the incidence of ILD was 3–5% with a mortality rate of 2–3%.[7,8] In contrast, outside of Japan, the rate of ILD was only 0.3%.[9] These reports suggested that the risk factors of ILD associated with gefitinib were male gender, a smoking history and a coincidence of idiopathic pulmonary fibrosis. However, the molecular mechanisms of ILD associated with gefitinib remain largely unknown.

Epidermal growth factor receptor is expressed on the surface of various cells and activates gene transcription, thus regulating cellular growth and differentiation. Although expression of EGFR is sparse in healthy adult human airways, including bronchial epithelial cells and alveolar type II cells, EGF signaling upregulates various gene transcriptions in these cells.[10,11] In alveolar type II cells, EGF signaling mediates cell differentiation and stimulates surfactant protein (SP)-A production.[12] Pulmonary surfactant secreted from alveolar type II cells is a mixture of lipids and proteins, and prevents the alveoli from collapsing at the end of expiration.[13,14] Ten percent of surfactant is composed of proteins, including hydrophilic SP-A and -D, and the hydrophobic proteins SP-B and SP-C.[15] Although SP-B and SP-C are critical for reduction of alveolar surface tension, SP-A and -D belong to the collectin subgroup of the C-type lectin superfamily in which lectin domains are associated with collagenous structures along with SP-D and mannose-binding lectin.[16,17]

Surfactant protein A is a multifunctional protein involved in maintenance surfactant homeostasis, lipid sorting, tubular myelin formation and innate immune defense in the lung. SP-A knockout mice reveal significant defects in host defense; SP-A$^{-/-}$ mice show impaired microbial clearance after intratracheal administration of group B *Streptococcus*,[18] *Haemophilus influenza*,[19] *Pseudomonas aeruginosa*,[20] *Pneumocystis carinii*,[21] and respiratory syncytial virus.[22] In addition, SP-A directly protects surfactant phospholipids and macrophages from oxidative damage.[23]

In this study, we hypothesized that the EGFR-TKI gefitinib inhibits the expression of SP-A on the alveolar type II cells and thus increases the susceptibility to pathogens.

Materials and Methods

Gefitinib treatment and Western blotting of EGFR on H441 cells. We used human lung adenocarcinoma H441 cells instead of alveolar type II cells because H441 cells stably express surfactant proteins *in vitro* and harbor wild-type *EGFR* gene.[24,25] H441 cells were cultured in RPMI-1640 medium with 10% fetal bovine serum. H441 grown in serum-free RPMI-1640 medium ± 20 μg/mL recombinant epidermal growth factor (EGF; Biomedical Technologies, Stoughton, MA, USA) were treated for 48 h with 1 μM gefitinib (AstraZeneca, UK).

After 48 h treatment with 1 μM gefitinib, the H441 cells were lysed in RIPA buffer containing protease inhibitors (Roche Molecular Biochemicals, Indianapolis, IN, USA) and 1 mM NaVO3 (Sigma, St Louis, MO, USA). After determination of protein concentration using the Bio-Rad Bradford protein assay (Bio-Rad

[6]To whom correspondence should be addressed. E-mail: yasosj@cc.hirosaki-u.ac.jp

doi: 10.1111/j.1349-7006.2008.00857.x

Laboratories, Hercules, CA, USA), 30 μg of total protein was loaded per lane on a 10% Bis-Tris Gel (Invitrogen, Carlsbad, CA, USA), and transferred to a PVDF membrane (Invitrogen). The membrane was incubated with rabbit antihuman EGFR (1005) Antibody (Santa Cruz Biotechnology, Santa Cruz, CA, USA) or mouse antiphospho-EGFR monoclonal antibody (YTyr1173; Upstate Biotechnologies, Lake Placid, NY, USA). The blots were stained with secondary antibody (goat antirat IgG-HR or rat antimouse IgG-HR; Santa Cruz Biotechnology) and the detection of specific signals was performed using the ECL Detection System (Amersham Pharmacia Biotech AB, Uppsala, Sweden).

Reverse transcription polymerase chain reaction of SP-A, -B, -C and -D and immunohistochemistry of SP-A on PC-3 cells. The total RNA (2 μg) extracted from the H441 cells treated with 1 μM gefitinib was converted into cDNA by Oligo(dT)12–18 primers and Superscript II reverse transcription (Gibco BRL, Carlsbad, CA, USA) in a final volume of 20 μL. Of this cDNA, 1 μL was amplified with the following sense and antisense primers, respectively: SP-A, 5′-gAAggACgTTTgTgTTggAA-3′ and 5′-TggATTCCTTgggACAgCAA-3′; SP-B, 5′-TACTCCgTCATCCTgCTCgA-3′ and 5′-gCTgCTCCACAAATTgCTTg-3′; SP-C, 5′-AgCAAAgAggTCCTgATggA-3′ and 5′-CTATTgAgAgCCTCAAgACT-3′; SP-D, 5′-AgCTgggCCCAAAggAgAAgTAgg-3′ and 5′-AgCggCAgAgCgTggAgAgg-3′; EGFR, 5′-CTTCTTgCAgCgATACAgCTC-3′ and 5′-ATgCTCCAATAAATTCACTgC-3′; and b-action, 5′-CTCTTTgATgTCACgCACgATTTC-3′ and 5′-gTgggCCgCTCTAggCACCAA-3′.

The amplification profile was 95°C for 5 min, 40 cycles of 94°C for 1 min, 60°C for 90 s and 72°C for 2 min.

H441 cells cultured on the slide glass with/without 1 μM gefitinib for 48 h were fixed with 4% buffered formaldehyde, and stained with the mouse antihuman SP-A antibody (clone PE-10; DAKO, San Diego, CA, USA) at ×50 dilution. The cells were then incubated with the avidin–biotin–peroxidase complex method Envision+System (DAKO).

***In vivo* experiments.** All animal experiments were approved by the institutional review board for animal experiments of Tohoku University. Female C57BL/6 mice purchased from Japan Charles River (Atsugi, Japan) were given a daily dose of 200 μL 1% Tween 80 (Sigma) solution p.o. containing either gefitinib (200 mg/kg) or no drug (control).

After 1 week, mice treated with gefitinib were instilled intratracheally with 250 μg/kg (5 μg/mouse) *Escherichia coli* lipopolysaccharide (LPS) 055:B5 (Sigma). To determine the response of SP-A to the lung injury, human SP-A (3 μg in 50 μL of phosphate-buffered saline/mouse), obtained from patients with alveolar proteinosis,[26] was administered intranasally on days 1–3 following the intratracheal LPS administration (5 μg/mouse).[27]

Bronchoalveolar lavage and Western blotting of SP-A and -D in the bronchoalveolar lavage fluid. Mice were subjected to brief anesthesia with i.p. injection of ketamine and xylazine. After loss of consciousness, the trachea was exposed with a midline incision and cannulated with a 24-G catheter. After the mice were killed by exsanguination, the lungs were lavaged three times with sterile 0.9% NaCl at a volume of 0.7 mL/wash. The average fluid recovery was greater than 80%. The bronchoalveolar lavage (BAL) fluid was centrifuged at 500 *g* for 10 min at 4°C and the supernatants were stored at –20°C until analysis.

Cells from BAL samples were resuspended in 1 mL normal saline. The cell differentials were performed on slides prepared in a Cytospin 3 (Shandon, Pittsburgh, PA, USA) centrifuged at a speed of 150 *g* for 2 min and stained with a modified Wright-Giemsa technique (Diff-Quik; Dade Behring, Dudingen, Switzerland).

Western blots of SP-A and -D in the BAL fluid were performed as described above using the rabbit antihuman SP-A polyclonal antibody and the rabbit antimouse SP-D polyclonal antibody Anti-Surfactant D (Chemicon International). Loading of BAL fluid was normalized by an amount of protein (25 μg/lane). The relative amount of immunoreactive SP-A present in each sample was quantitated by NIH Image (National Institute of Mental Health). The densitometric data from each blot were normalized to the control condition with the control value set equal to one for each experiment.

Enzyme-linked immunosorbent assay for tumor necrosis factor-α. Tumor necrosis factor (TNF)-α concentrations in BAL fluid and plasma were determined using a specific enzyme-linked immunosorbent assay TNF-α ELISA Kit (BioSource International, Camarillo, CA, USA) in conjunction with a Bio-Rad model 550 microplate reader with accompanying software (Bio-Rad, Hercules, CA, USA) as directed by the manufacturer. The ELISA had a lower detection limit of 3 pg/mL.

Histopathology of the lung. After thoracotomy, the left lung was inflated with 4% phosphate-buffered formalin (pH 7.4) at a pressure of 20 cm H_2O through the trachea for 6 h and subsequently fixed in 15% phosphate-buffered formalin for 24 h. After paraffin embedding, 4-μm sections were cut and stained with hematoxylin–eosin (HE) for histological analysis.

Statistics. Data are expressed as means ± standard error (SE). Statistical analysis was performed with StatView (SAS Institute). ANOVA was used to determine differences among experimental groups. The Student–Newman–Keuls test was used for a multiple comparison. $P < 0.05$ was considered significant.

Results

Suppression of *SP-A* by gefitinib treatment on H441 cells. A dose–response curve to 72 h treatment of gefitinib on H441 cells revealed that IC_{50} was 20 μM. Treatment with 1 μM gefitinib did not significantly inhibit H441 cell growth (data not shown). Treatment with 1 μM gefitinib completely blocked the EGF-induced autophosphorylation of EGFR in H441 cells (Fig. 1a, upper panel), whereas the level of whole EGFR protein was not changed by gefitinib treatment (Fig. 1a, lower panel). EGF increased autophosphorylation of EGFR. This result implied that treatment with 1 μM gefitinib completely blocked the EGF signaling in H441 cells. The expression level of surfactant proteins on H441 cells after gefitinib treatment was examined because previous reports had suggested a relationship between EGF signaling and surfactant proteins. The level of *SP-A* mRNA was suppressed by gefitinib treatment in serum-free medium plus 20 μg/mL EGF conditions, whereas *SP-B*, *-C* and *-D* expression levels did not change after gefitinib treatment (Fig. 1b). Immunohistochemistry also revealed strong suppression of SP-A protein after gefitinib treatment (Fig. 1c). SP-A protein could not be detected by Western blotting, possibly because of the low expression of SP-A in H441 cells.

Suppression of SP-A in BAL fluid of gefitinib-treated mice. The examination of SP-A and -D in BAL fluid revealed that gefitinib gradually suppressed the SP-A level, and SP-A was suppressed by 68% by day 8 (Fig. 2a,b) ($P < 0.01$). The level of SP-D in BAL fluid did not change throughout the gefitinib treatment period (Fig. 2a,b). The intratracheal instillation of LPS to gefitinib-treated mice was conducted to assess the effect of gefitinib on inflammation induced by bacterial infection. In control mice, LPS instillation increased the level of SP-A in BAL fluid by 42% after 72 h and declined after peak, suggesting an anti-inflammatory response of SP-A. However, although the SP-A level in BAL fluid in gefitinib-treated mice was increased after LPS instillation, the level of SP-A was significantly lower than control at 24 and 72 h after LPS instillation (Fig. 3a,b). Although we found lower levels of SP-A in BAL fluid after gefitinib treatment, SP-A immunohistochemistry of the lung did not show any change of staining intensity (data not shown). We suppose that expression level of SP-A after gefitinib treatment was high enough for staining. In contrast, increases of SP-D after LPS instillation were of similar levels in both control and gefitinib-treated mice.

doi: 10.1111/j.1349-7006.2008.00857.x

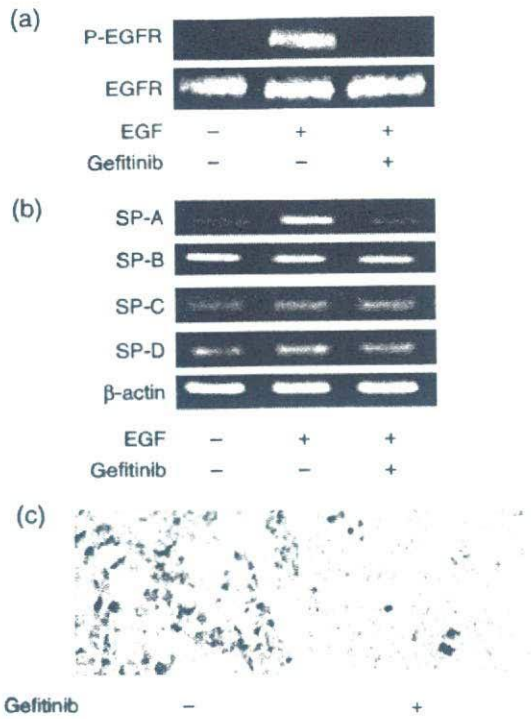

Fig. 1. Autophosphorylation of epidermal growth factor receptor (EGFR) and expression levels of surfactant proteins (SP)-A, -B, -C and -D in H441 cells. H441 cells cultured in serum-free RPMI-1640 medium plus 20 μg/mL EGF were treated with 1 μM gefitinib for 48 h. (a) Western blotting of whole EGFR protein and autophosphorylated EGFR protein in H441 cells after gefitinib treatment. (b) Reverse transcription polymerase chain reaction of *SP-A*, *-B*, *-C* and *-D* in H441 cells after gefitinib treatment. (c) Immunohistochemistry of SP-A on H441 cells after gefitinib treatment. P-EGFR, .

Gefitinib treatment exacerbates LPS-induced lung inflammation. LPS was administered intratracheally to mice following 1 week of gefitinib treatment in order to assess whether pretreatment with gefitinib increases the susceptibility of lung inflammation by LPS. The cell density of BAL fluid remained at a high level on day 6 in gefitinib-pretreated mice, but improved to a normal level in control mice (Fig. 4a). The percentage of neutrophils in BAL fluid of gefitinib-pretreated mice (13.5%) remained higher than control mice (6.0%) on day 6 (Table 1). Histopathological examination of the lung section also revealed that gefitinib pretreated mice showed stronger inflammatory infiltrates, mainly consisting of neutrophils (Fig. 4b). Neither gefitinib alone nor

Table 1. Percentage of alveolar macrophages and neutrophils in bronchoalveolar lavage fluid

Days after LPS	Gefitinib	LPS	SP-A	Macrophages (%)	Neutrophils (%)
0	–	–	–	93.3 ± 0.3	2.1 ± 0.3
0	+	–	–	89.0 ± 1.5	6.9 ± 1.1
3	–	+	–	34.1 ± 5.5	61.0 ± 6.3
3	+	+	–	21.6 ± 2.4	72.5 ± 3.3
3	+	+	+	43.0 ± 1.6	40.7 ± 1.8**
6	–	+	–	77.3 ± 2.8	6.0 ± 0.3
6	+	+	–	81.1 ± 0.6	13.5 ± 1.1
6	+	+	+	84.6 ± 3.6	1.3 ± 0.5*

*$P < 0.05$ (compared with gefitinib+/LPS + mice); **$P < 0.01$ (compared with gefitinib+/LPS + mice). BAL, bronchoalveolar lavage; LPS, lipopolysaccharide; SP, surfactant protein.

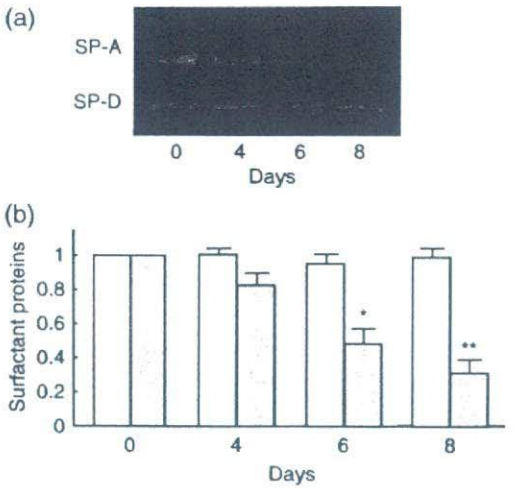

Fig. 2. Contents of surfactant proteins (SP)-A and -D in bronchoalveolar lavage (BAL) fluid after gefitinib treatment. (a) Western blotting and (b) densitometric data of SP-A and -D in BAL fluid from mice at 0, 4, 6 and 8 days treatment with or without gefitinib (200 mg/kg). The values were normalized to the control condition for each experiment. (□) SP-D; (grey) SP-A. Data presents means ± standard error in five mice. *$P < 0.05$, **$P < 0.01$.

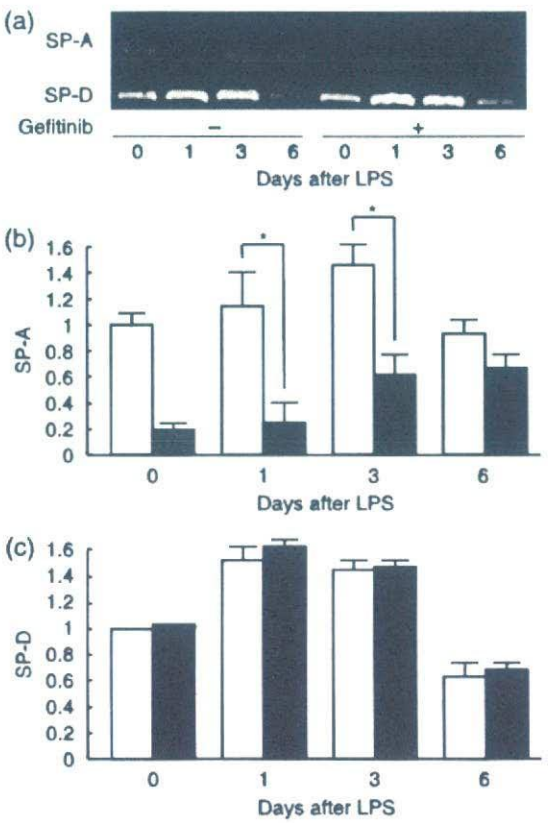

Fig. 3. Surfactant protein-A levels after lipopolysaccharide (LPS) instillation in the bronchoalveolar lavage (BAL) fluid. (a) Western blotting of SP-A and -D and densitometric data of (b) SP-A and (c) SP-D in BAL fluid from mice with/without 7 days gefitinib pretreatment, 72 h after the intratracheal LPS instillation (250 μg/kg). (□) mice receiving LPS only; (■) mice receiving gefitinib and LPS. Data presents means ± standard error in five mice. *$P < 0.05$.

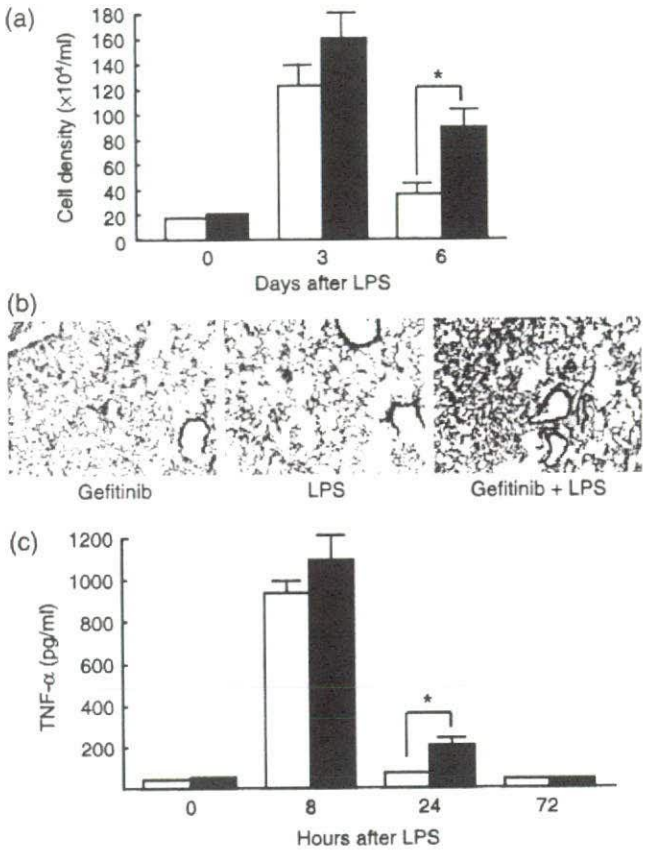

Fig. 4. Lipopolysaccharide (LPS)-induced inflammatory change *in vivo*. (a) Cell density in bronchoalveolar lavage (BAL) fluid from mice with/without gefitinib pretreatment, 6 days after intratracheal LPS instillation. (b) Infiltration of inflammatory cells 3 days after LPS instillation in the lungs of mice treated with gefitinib only (left), with LPS only (middle), or with gefitinib and LPS (right). (c) Tumor necrosis factor (TNF)-α enzyme-linked immunosorbent assay was performed on mouse BAL fluid 8, 24 and 72 h after the intratracheal LPS instillation ($n = 6$). (□) mice receiving LPS only; (■) mice receiving gefitinib and LPS. Data presents means ± standard error (SE) in five mice. $*P < 0.05$.

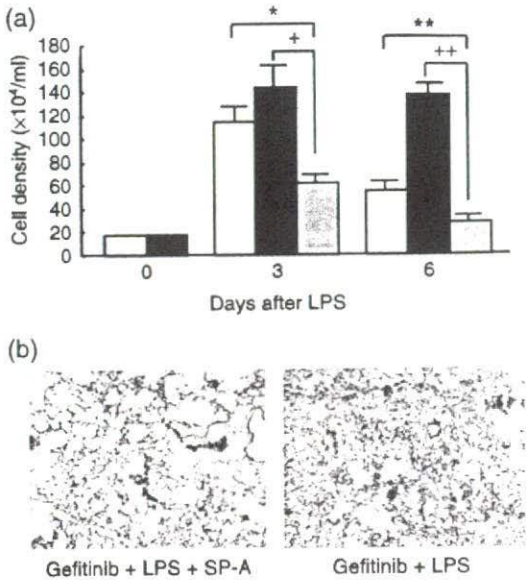

Fig. 5. Effects of surfactant protein (SP)-A rescue on lipopolysaccharide (LPS)-induced lung inflammation. (a) Mice with/without gefitinib pretreatment received intratracheal LPS instillation on day 1 and SP-A (150 μg/kg) on days 1–3. BAL was performed on days 3 and 6 after LPS instillation. (□) control mice; (■) mice treated with gefitinib only (grey) mice treated with gefitinib and rescued by SP-A or gefitinib+/LPS + group. Data presents means ± standard error in three mice. $*P < 0.05$, $**P < 0.01$. (b) Lung tissue (HE) 3 days after LPS instillation in the SP-A treated group (left) and control group (gefitinib + LPS) (right).

LPS alone induced the neutrophil accumulation in the lung 3 days after the treatment (Fig. 4b).

Although the level of inflammatory cytokine TNF-α in BAL fluid was drastically increased 8 h after the administration of LPS in both groups of mice, gefitinib pretreated mice retained a detectable level of TNF-α 24 h after LPS administration (Fig. 4c). TNF-α could not be detected in the plasma of both control and gefitinib-treated mice after LPS instillation (data not shown). These data suggest that gefitinib pretreatment prolonged the lung inflammatory response to LPS.

SP-A rescue inhibits exacerbation of LPS-induced inflammation *in vivo*. The effect of rescue SP-A on lung inflammation induced by LPS in gefitinib-pretreated mice was examined. The cell density of BAL fluid in the gefitinib pretreated mice was decreased by SP-A rescue on both days 3 and 6 (Fig. 5a). SP-A rescue also inhibited the increase of neutrophils induced by LPS in gefitinib-treated mice on days 3 and 6 (Table 1). Histological assessment also showed that SP-A administration significantly improved the neutrophil accumulation in the lung (Fig. 5b).

Discussion

The present study demonstrated that mice pretreated with gefitinib had exacerbated LPS-induced lung inflammation, and that this exacerbation was due to the suppression of SP-A expression in the lung. It was also demonstrated *in vitro* that gefitinib treatment of human lung adenocarcinoma H441 cells suppressed the expression of SP-A. These results suggest that ILD observed in patients treated with gefitinib may be, at least in part, associated with the suppression of SP-A expression by gefitinib.

Gefitinib, an EGFR-TKI, has been shown to be effective for the treatment of advanced NSCLC with a favorable adverse event profile in phase I and II trials,[1,2,28] Shortly after the approval of gefitinib for the treatment of inoperable and recurrent NSCLC, a number of cases were reported of ILD after gefitinib treatment.[6–8] Major risk factors of ILD were a smoking history, pre-existing or concurrent idiopathic pulmonary fibrosis, and poor performance status. Although the existence of ILD associated with gefitinib has been seen in clinics, the mechanism of ILD associated with gefitinib has not been fully elucidated.

This study has shown that the expression of *SP-A* mRNA is regulated by EGF signaling in human adenocarcinoma H441 cells, whereas *SP-B*, *-C* and *-D* are not. SP-A levels in BAL fluid were also reduced in mice treated with gefitinib. These results revealed that SP-A expression in human type II alveolar cells could be regulated by the EGF signal.

Pulmonary surfactant proteins are synthesized specifically by alveolar type II cells and bronchioalveolar Clara cells, and are positively or negatively regulated by various factors such as glucocorticoids, retinoids, insulin, growth factors and cytokines.[29] Among these regulatory factors, EGF positively regulates SP-A, a major constituent of the surfactant. EGF accelerates alveolarization and decreases the severity of respiratory syndromes in fetal lambs.[30] Blockade of EGF signaling by the EGFR-TKI, genistein and tyrphostin, inhibited SP-A expression in cultured fetal lung explants.[31] Antisense oligonucleotide against *EGFR* mRNA inhibited *SP-A* expression in human fetal lung tissue during alveolar type II differentiation.[32] Mechanisms of different

doi: 10.1111/j.1349-7006.2008.00857.x

effects of EGFR-TKI on expression among *SP-A* and *-B*, *-C* and *SP-D* are still unclear. Although precise mechanisms of *SP-A* expression have been studied,[29] regulatory mechanisms of *SP-B*, *-C* and *-D* are warranted. In this context, it could be suggested that treatment with EGFR-TKI reduces *SP-A* expression in the human adult lung.

Pathogen-derived components, such as LPS derived from Gram-negative bacteria and peptideglycan derived from Gram-positive bacteria, are potent stimulators of inflammation. SP-A interacts with CD14 on alveolar macrophages and inhibits the binding of smooth LPS to CD14 and reduces TNF-α expression induced by LPS.[33] Therefore, SP-A$^{-/-}$ mice show significantly enhanced TNF-α production induced by smooth LPS.[34] TNF-α production induced by peptideglycan was also inhibited by SP-A.[35] These previous studies are in agreement with our results. Pre-treatment with gefitinib exacerbates LPS-induced lung inflammation in mice, and this exacerbation could be rescued by the administration of SP-A.

Among the several risk factors for ILD in clinical studies, smoking history and interstitial pulmonary fibrosis are linked to a reduced expression of SP-A in the lung. Betsuyaku *et al.* reported that aging alone or combined with long-term smoking leads to a decrease of SP-A levels in the lungs of human subjects.[36] The concentration of SP-A in the BAL fluid of patients with idiopathic pulmonary fibrosis was lower than in control subjects.[37,38] Tamura *et al.* retrospectively analyzed baseline SP-A expression levels of cancer tissues and normal bronchial tissues by immunohistochemistry from 20 NSCLC patients treated with gefitinib; 10 patients developed ILD after gefitinib treatment and 10 patients did not.[39] They found that baseline SP-A expression levels in both cancer and normal tissues was significantly lower in patients with ILD than in patients without ILD. They concluded that baseline SP-A expression could be a predictive marker for ILD by gefitinib. Although the present study and that by Suzuki *et al.* used a larger dose of gefitinib (200 mg/kg/day) than that used in humans (1–14 mg/kg/day [50–700 mg/body/day]),[40] we observed that a lower dose of gefitinib (25 mg/kg) equally suppressed SP-A expression in mice (data not shown). Combined with these clinical findings and this present study in mice, it could be speculated that human subjects with low expression levels of SP-A due to smoking or idiopathic pulmonary fibrosis become susceptible to lung damage by pathogens, oxidative stress or other factors.

Suzuki *et al.* reported that, in mice, treatment with gefitinib exacerbated the pulmonary fibrosis induced by bleomycin because *EGF* and *EGFR* were upregulated early in the response to lung injury.[40,41] These findings suggest that inhibition of EGFR signaling by gefitinib impairs the repair of and, thereby, exacerbates pulmonary injury, especially in patients with pulmonary comorbidities.

Although ILD associated with gefitinib in Japanese patients has been reported in Japan at a prevalence of 3–5%,[7,8] the prevalence of ILD among gefitinib-treated patients in the USA and Europe was less than 1%.[42,43] The reason for the different prevalence of ILD associated with gefitinib between Japan and Western countries remains unclear. It might be attributable to Japanese patients having an increased genetic susceptibility to ILD.

In conclusion, we have demonstrated that pretreatment with gefitinib exacerbates LPS-induced lung inflammation by reducing levels of SP-A. These findings suggest that ILD after EGFR-TKI treatment may be related in part to a reduction of SP-A.

Acknowledgments

This study was supported by the Smoking Research Foundation in Japan (2003–2005) and the Public Trust Haraguchi Memorial Cancer Research Fund (2005).

References

1 Fukuoka M, Yano S, Giaccone G *et al.* Multi-institutional randomized phase II trial of gefitinib for previously treated patients with advanced non-small-cell lung cancer (The IDEAL 1 Trial). *J Clin Oncol* 2003; **21**: 2237–46.
2 Kris MG, Natale RB, Herbst RS *et al.* Efficacy of gefitinib, an inhibitor of the epidermal growth factor receptor tyrosine kinase, in symptomatic patients with non-small cell lung cancer: a randomized trial. *JAMA* 2003; **290**: 2149–58.
3 Miller VA, Kris MG, Shah N *et al.* Bronchioloalveolar pathologic subtype and smoking history predict sensitivity to gefitinib in advanced non-small-cell lung cancer. *J Clin Oncol* 2004; **22**: 1103–9.
4 Paez JG, Janne PA, Lee JC *et al.* EGFR mutations in lung cancer: correlation with clinical response to gefitinib therapy. *Science* 2004; **304**: 1497–500.
5 Lynch TJ, Bell DW, Sordella R *et al.* Activating mutations in the epidermal growth factor receptor underlying responsiveness of non-small-cell lung cancer to gefitinib. *N Engl J Med* 2004; **350**: 2129–39.
6 Inoue A, Saijo Y, Maemondo M *et al.* Severe acute interstitial pneumonia and gefitinib. *Lancet* 2003; **11** (361): 137–9.
7 Ando M, Okamoto I, Yamamoto N *et al.* Predictive factors for interstitial lung disease, antitumor response, and survival in non-small-cell lung cancer patients treated with gefitinib. *J Clin Oncol* 2006; **24** (16): 2549–56.
8 Takano T, Ohe Y, Kusumoto M *et al.* Risk factors for interstitial lung disease and predictive factors for tumor response in patients with advanced non-small cell lung cancer treated with gefitinib. *Lung Cancer* 2004; **45** (1): 93–104.
9 Forsythe B, Faulkner K. Overview of the tolerability of gefitinib (IRESSA®) monotherapy. Clinical experience in non-small cell lung cancer. *Drug Saf* 2004; **27**: 1081–92.
10 Takeyama K, Dabbagh K, Lee HM *et al.* Epidermal growth factor system regulates mucin production in airways. *Proc Natl Acad Sci USA* 1999; **96** (6): 3081–6.
11 Takeyama K, Fahy JV, Nadel JA. Relationship of epidermal growth factor receptors to goblet cell production in human bronchi. *Am J Respir Crit Care Med* 2001 Feb; **163** (2): 511–16.
12 Whitsett JA, Weaver TE, Lieberman MA, Clark JC, Daugherty C. Differential effects of epidermal growth factor and transforming growth factor-beta on synthesis of Mr = 35 000 surfactant-associated protein in fetal lung. *J Biol Chem* 1987; **262**: 7908–13.
13 King RJ, Clements JA. Surface active materials from dog lung. I. Method of isolation. *Am J Physiol* 1972; **223**: 707–14.
14 King RJ, Clements JA. Surface active materials from dog lung. II. Composition and physiological correlations. *Am J Physiol* 1972; **223**: 715–26.
15 Kuroki Y, Voelker DR. Pulmonary surfactant proteins. *J Biol Chem* 1994; **269**: 25943–6.
16 Sano H, Kuroki Y. The lung collectins, SP-A and SP-D, modulate pulmonary innate immunity. *Mol Immunol* 2005; **42**: 279–87.
17 Wright JR, Borron P, Brinker KG, Folz RJ. Surfactant protein A regulation of innate and adaptive immune responses in lung inflammation. *Am J Respir Cell Mol Biol* 2001; **24**: 513–7.
18 LeVine AM, Bruno MD, Huelsman KM, Ross GF, Whitsett JA, Korfhagen TR. Surfactant protein A-deficient mice are susceptible to group B streptococcal infection. *J Immunol* 1997; **1** (158): 4336–40.
19 LeVine AM, Whitsett JA, Gwozdz JA *et al.* Distinct effects of surfactant protein A or D deficiency during bacterial infection on the lung. *J Immunol* 2000; **165**: 3934–40.
20 LeVine AM, Kurak KE, Bruno MD, Stark JM, Whitsett JA, Korfhagen TR. Surfactant protein-A-deficient mice are susceptible to Pseudomonas aeruginosa infection. *Am J Respir Cell Mol Biol* 1998; **19**: 700–8.
21 Linke MJ, Harris CE, Korfhagen TR *et al.* Immunosuppressed surfactant protein A-deficient mice have increased susceptibility to *Pneumocystis carinii* infection. *J Infect Dis* 2001; **183**: 943–52.
22 LeVine AM, Gwozdz J, Stark J, Bruno M, Whitsett J, Korfhagen T. Surfactant protein-A enhances respiratory syncytial virus clearance *in vivo*. *J Clin Invest* 1999; **103**: 1015–21.
23 Bridges JP, Davis HW, Damodarasamy M *et al.* Pulmonary surfactant proteins A and D are potent endogenous inhibitors of lipid peroxidation and oxidative cellular injury. *J Biol Chem* 2000; **275**: 38848–55.
24 Fukazawa T, Maeda Y, Durbin ML *et al.* Pulmonary adenocarcinoma-targeted gene therapy by a cancer- and tissue-specific promoter system. *Mol Cancer Ther* 2007; **6**: 244–52.
25 Mukohara T, Engelman JA, Hanna NH *et al.* Differential effects of gefitinib and cetuximab on non-small-cell lung cancers bearing epidermal growth factor receptor mutations. *J Natl Cancer Inst* 2005; **97**: 1185–94.
26 Kuroki Y, Tsutahara S, Shijubo N *et al.* Elevated levels of lung surfactant protein A in sera from patients with idiopathic pulmonary fibrosis and pulmonary alveolar proteinosis. *Am Rev Respir Dis* 1993; **147**: 723–9.
27 Madan T, Kishore U, Singh M *et al.* Surfactant proteins A and D protect mice against pulmonary hypersensitivity induced by *Aspergillus fumigatus* antigens and allergens. *J Clin Invest* 2001; **107**: 467–75.

28 Nakagawa K, Tamura T, Negoro S *et al.* Phase I pharmacokinetic trial of the selective oral epidermal growth factor receptor tyrosine kinase inhibitor gefitinib ('Iressa', ZD1839) in Japanese patients with solid malignant tumors. *Ann Oncol* 2003; **14**: 922–30.
29 Mendelson CR. Role of transcription factors in fetal lung development and surfactant protein gene expression. *Annu Rev Physiol* 2000; **62**: 875–915.
30 Sundell HW, Gray ME, Serenius FS, Escobedo MB, Stahlman MT. Effects of epidermal growth factor on lung maturation in fetal lambs. *Am J Pathol* 1980; **100**: 707–25.
31 Klein JM, DeWild LJ, McCarthy TA. Effect of tyrosine kinase inhibition on surfactant protein A gene expression during human lung development. *Am J Physiol* 1998; **274** (4 Part 1): L542–51.
32 Klein JM, McCarthy TA, Dagle JM, Snyder JM. Antisense inhibition of epidermal growth factor receptor decreases expression of human surfactant protein A. *Am J Respir Cell Mol Biol* 2000; **22**: 676–84.
33 Sano H, Sohma H, Muta T, Nomura S, Voelker DR, Kuroki Y. Pulmonary surfactant protein A modulates the cellular response to smooth and rough lipopolysaccharides by interaction with CD14. *J Immunol* 1999; **163**: 387–95.
34 Borron P, McIntosh JC, Korfhagen TR, Whitsett JA, Taylor J, Wright JR. Surfactant-associated protein A inhibits LPS-induced cytokine and nitric oxide production *in vivo*. *Am J Physiol Lung Cell Mol Physiol* 2000; **278**: L840–7.
35 Murakami S, Iwaki D, Mitsuzawa H *et al.* Surfactant protein A inhibits peptidoglycan-induced tumor necrosis factor-alpha secretion in U937 cells and alveolar macrophages by direct interaction with toll-like receptor 2. *J Biol Chem* 2002; **277**: 6830–7.
36 Betsuyaku T, Kuroki Y, Nagai K, Nasuhara Y, Nishimura M. Effects of ageing and smoking on SP-A and SP-D levels in bronchoalveolar lavage fluid. *Eur Respir J* 2004; **24**: 964–70.
37 McCormack FX, King TE Jr, Voelker DR, Robinson PC, Mason RJ. Idiopathic pulmonary fibrosis. Abnormalities in the bronchoalveolar lavage content of surfactant protein A. *Am Rev Respir Dis* 1991; **144**: 160–6.
38 McCormack FX, King TE Jr, Bucher BL, Nielsen L, Mason RJ. Surfactant protein A predicts survival in idiopathic pulmonary fibrosis. *Am J Respir Crit Care Med* 1995; **152**: 751–9.
39 Tamura K, Okamoto I, Kurata T, Satoh T, Nakagawa K, Fukuoka M. Low expressions of surfactant-associated protein (SP-A) in cancer tissues or in normal bronchial epithelial cells by immuno-histochemistry predict interstitial lung diseases induced by gefitinib in patients with advanced non-small cell lung cancer. *Proc Am Soc Clin Oncol* 2005; **23**: 667s.
40 Suzuki H, Aoshiba K, Yokohori N, Nagai A. Epidermal growth factor receptor tyrosine kinase inhibition augments a murine model of pulmonary fibrosis. *Cancer Res* 2003; **63**: 5054–9.
41 Madtes DK, Busby HK, Strandjord TP, Clark JG. Expression of transforming growth factor-alpha and epidermal growth factor receptor is increased following bleomycin-induced lung injury in rats. *Am J Respir Cell Mol Biol* 1994; **11**: 540–51.
42 Giaccone G, Herbst RS, Manegold C *et al.* Gefitinib in combination with gemcitabine and cisplatin in advanced non-small-cell lung cancer: a phase III trial – INTACT 1. *J Clin Oncol* 2004; **22**: 777–84.
43 Herbst RS, Giaccone G, Schiller JH *et al.* Gefitinib in combination with paclitaxel and carboplatin in advanced non-small-cell lung cancer: a phase III trial – INTACT 2. *J Clin Oncol* 2004; **22**: 785–94.

doi: 10.1111/j.1349-7006.2008.00857.x

Eur Respir J 2006; 28: 1013–1019
DOI: 10.1183/09031936.06.00132505

Genetic linkage analysis of pulmonary fibrotic response to silica in mice

Y. Ohtsuka, X-T. Wang, J. Saito, T. Ishida and M. Munakata

ABSTRACT: Inter-individual variations in the development of silicosis, even within the same environments, have been reported, which suggest the contribution of genetic factors in silicosis aetiology. The aim of the present study was to determine whether there is any significant genetic influence on the development of silicosis. Furthermore, which genetic loci are responsible for the pulmonary response to silica exposure?

Eight strains of inbred mice were used to examine the genetic influence on the lung fibrotic response to silica exposure. After intercross-breeding between the most susceptible and most resistant strains, a genome-wide linkage analysis of quantitative trait loci (QTL) was performed. Hydroxyproline was applied as an index, and genotypes of 167 marker genes were analysed by fragment analysis using a capillary-type sequencer.

There was significant inter-strain difference in the mean concentration of hydroxyproline contents among the eight strains of mice. Breeding studies were conducted between the most susceptible, C57BL/6J, and the most resistant strain, CBA/J. A genome-wide linkage analysis of silica-exposed intercrossed cohorts identified significant QTL on chromosome 4 and suggestive QTL on chromosomes 3 and 18.

The present study demonstrates that genetic factors may play a significant role in fibrotic-lung responses to silica; one significant and two suggestive quantitative trait loci were identified.

KEYWORDS: C57BL/6J, CBA/J, hydroxyproline, intercross, quantitative trait locus

Silicosis is an occupational lung disease caused by inhalation of dust containing free crystalline silica. Free-silica is still an occupational fibrogenic hazard despite the technical adequacy of current protective equipment. In the USA, it was estimated that 200,000 miners and 1.7 million nonmining workers had occupational exposures to inhaled silica [1]. In the advanced stage, silicosis complicates tuberculosis, respiratory failure due to progressive massive fibrosis, emphysema, and lung cancer. Considerable attention has been paid to these adverse effects of silica dusts.

Concerning the development of silicosis, extrinsic factors such as duration, amount of exposure, and content of free crystalline silica have been known as critical determinants of the progression of silicosis [2]. However, some of the intrinsic (genetic) factors that may influence susceptibility to silicosis have been reported. Associations of specific human leukocyte antigen (HLA) haplotype with silicosis have been reported in a Japanese population [3]. In a German population, HLA haplotype association with coal worker's pneumoconiosis has also been reported [4]. Associations of gene polymorphisms of pro-inflammatory cytokines (*e.g.* tumour necrosis factor-α, interleukin-1 receptor) have been reported [5–7]. In addition to these epidemiological studies, the present authors clarified the importance of genetic background on the variation in inflammation and fibrotic response in a murine silicosis model [8, 9].

The objective of the current study was to identify, using inbred mice, the genetic basis for susceptibility to silica-induced pulmonary fibrosis. Inbred mice provide a well-characterised animal model for understanding genetic and environmental factors that determine susceptibility to complex disease processes. Furthermore, the mouse is accepted as an excellent model of human disease processes because there is extensive linkage homology between the mouse and human genomes.

Any genetic influence on the inflammatory and fibrotic response to silica was examined in eight strains of inbred mice. A genome-wide search for genes responsible for silicosis was also conducted in the present model. The current study reports significant genetic influence on the fibrotic response among eight strains of mice compared

AFFILIATIONS
Dept of Pulmonary Medicine, School of Medicine, Fukushima Medical University, Fukushima, Japan.

CORRESPONDENCE
Y. Ohtsuka
Dept of Internal Medicine
Iwamizawa Rosai Hospital
4-jyo
Higashi 16-chome 5
Iwamizawa
Hokkaido 068-0004
Japan
Fax: 81 126221304
E-mail: yohtsuka@kvf.biglobe.ne.jp

Received:
November 11 2005
Accepted after revision:
June 29 2006

SUPPORT STATEMENT
The present study was supported by research grants from the Ministry of Education, Science and Culture, Japan (No. 13470129).

European Respiratory Journal
Print ISSN 0903-1936
Online ISSN 1399-3003

with titanium dioxide (TiO_2)-instilled control, and the linkage analysis of intercrossed (F2) mice identified significant quantitative trait loci (QTL) on chromosome 4 and suggestive QTL on chromosomes 3 and 18. Some of the results of the current study have been previously reported [9].

MATERIALS AND METHODS

Animals

Male (6–8 week old) mice of the following inbred strains were purchased from Sankyo Labo Service (Tokyo, Japan) and Clea Japan Inc. (Tokyo, Japan): A/J, AKR/J, Balb/cJ, C3H/HeJ, C57BL/6J, C57BL/10J, CBA/J, and DBA/2J. Breeding studies between the most susceptible and most resistant strains of mice were conducted. The following crosses were generated: male F1 were bred with females of the most susceptible strain to produce backcross progeny; F1 were intercrossed to produce F2 progeny. Progeny were weaned at 4 weeks of age, separated according to sex and housed in micro-isolation cages until they reached the appropriate age for experimentation (6–8 weeks). The mice were handled in accordance with the Helsinki convention and the standards established by the Animal Welfare Acts set forth by Fukushima Medical University guidelines.

Study design

Inter-strain comparison

Mice of all eight strains aged 6–8 weeks were anesthetised with *i.p.* pentobarbital and their trachea exposed surgically. Prepared silica (0.2 $g \cdot kg^{-1}$ in 50 $mg \cdot mL^{-1}$ saline) was instilled intratracheally, as described in previously [8]. The control animals in each strain were given 0.2 $g \cdot kg^{-1}$ of inert TiO_2 (50 $mg \cdot mL^{-1}$ saline) intratracheally. Twenty-eight days after intratracheal silica instillation, pathological fibrosis indices were evaluated using estimates by ASHCROFT *et al.* [10], and hydroxyproline content per lung was also assessed.

Linkage analysis

Intercross (F2) mice (6–8 weeks old) were anesthetised and exposed to silica as described above. As a control, three mice of the most susceptible strain were given 0.02 mL of intratracheal saline in each experiment. Twenty-eight days after silica instillation, collagen deposition of the right lung in each mouse was assayed and the kidneys taken for DNA extraction.

Collagen assay

Collagen deposition was estimated by determining the total hydroxyproline content of the left lung. Hydroxyproline was measured according to a method by WOESSNER [11] as reported previously [8]. Results were calculated as micrograms hydroxyproline per lung ($\mu g \cdot lung^{-1}$), and expressed as the ratio of the mean value of control mice in each experiment.

Morphological evaluation of lung sections

The right lungs were fixed, embedded in paraffin, sectioned horizontally to include most of the parenchyma at 4 μm, and stained with haematoxylin-eosin. The sections were scanned, by an observer blind to treatment, to determine the degree of fibrosis in 30 fields per sample at 100× magnification and analysed semi-quantitatively according to the method by ASHCROFT *et al.* [10]. Values of the samples were expressed as a fibrosis index, the mean grade of fibrosis per field.

DNA extraction and genotyping

DNA was extracted from a kidney of each phenotyped animal and prepared for PCR. PCR reactions were run in 96-well plates with 15.0 μL total volume consisting of: 1 μL DNA (4 ng); 1.5 μL 10× reaction buffer; 1.5 μL 25 mM $MgCl_2$; 1.5 μL 2.5 mM deoxynucleotide triphosphates (equal mixture of deoxy-adenosine, -cytidine, -guanosine and -thymidine triphosphates); 0.3 μL 10 mM primers (Applied Biosystems, Foster city, CA, USA); 0.6 U Taq polymerase; and brought to volume with distilled water. Primers for simple sequence-length polymorphisms (SSLPs) that differed between C57BL/6J and CBA/J progenitors were chosen from a website [12].

PCR amplification consisted of 10 cycles (94°C for 15 s, 55°C for 15 s and 72°C for 30 s) preceded by a denaturation step of 94°C for 12 min, and followed by 20 cycles (89°C for 15 s, 55°C for 15 s, and 72°C for 30 s) and a final elongation step for 10 min at 72°C. Pooled PCR product was mixed with 310 Genetic analyser standard solution (Gene Scan 400HD ROX 0.5μL, deionised formamide 12μL), and denatured at 95°C for 2 min. This sample was quickly chilled on ice until loading on the machine. The treated PCR products were analysed by ABI PRISM 310 Genetic Analyser with the Gene Scan program (Applied Biosystems).

Statistical analysis of inter-strain comparison

The effects of exposure (silica *versus* TiO_2) and strain on pulmonary responses were assessed by two-way ANOVA [13]. Tukey's test was used for *a posteriori* comparisons of means. In *a posteriori* comparison of hydroxyproline content among silica-exposed C57BL/6J, CBA/J, and B6CBAF1/J mice, Dunnett's T3-test was used because of the different number of mice in each group [13]. The strain distribution patterns (SDPs) for lung responses to silica were compared with the SDPs for silica by nonparametric Spearman rank-correlation. Significance was accepted at $p<0.05$.

Linkage analysis

A scan of the entire genome was completed by genotyping 25 phenotypically high-responder (n=13) and nonresponder (n=12) mice from a total population of 117 F2 mice [13]. Interval analyses were performed for each SSLP marker and at 10-centimorgan intervals between SSLPs. The dominance properties of each putative QTL were evaluated by performing interval analyses using free, additive, recessive, and dominant regression models. The regressions and significance of each association, likelihood ratio Chi-squared statistic, were calculated. Putative QTLs were further analysed by including the entire F2 cohort within the chromosomes identified by selective genotyping. Permutation tests were performed on the phenotype and the genotype data to establish empirically the significance thresholds of all QTL mapping results, using Map Manager QTX [14] and following the methods of CHURCHILL and DOERGE [15]. For the genome scan, 10,000 permutations were performed to establish significant and suggestive linkage threshold values. These values correspond to the genome-wide probabilities proposed by LANDER and KRUGLYAK [16].

RESULTS

Hydroxyproline content per lung and pathological fibrosis indices were used as indicators of lung fibrosis. ANOVA of

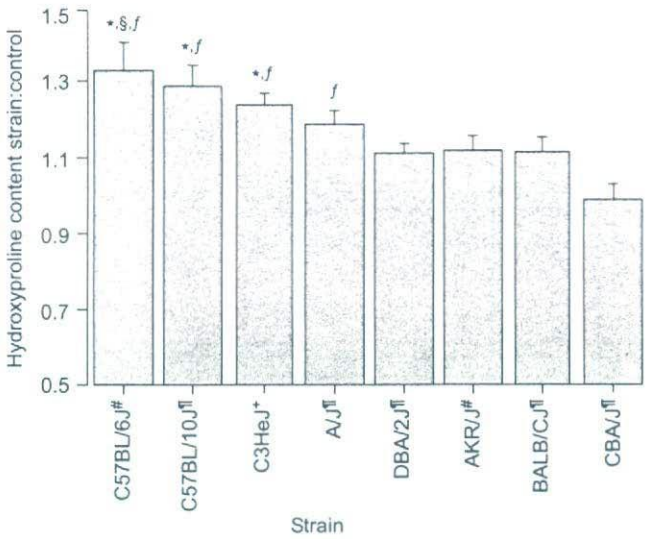

FIGURE 1. The ratio of lung hydroxyproline content in eight mice strains 28 days after intratracheal silica instillation. Data are presented as mean+SE. #: n=8; ¶: n=12; +: n=16; §: significantly different to Balb/cJ; f: significantly different to CBA; *: $p<0.05$ *versus* control.

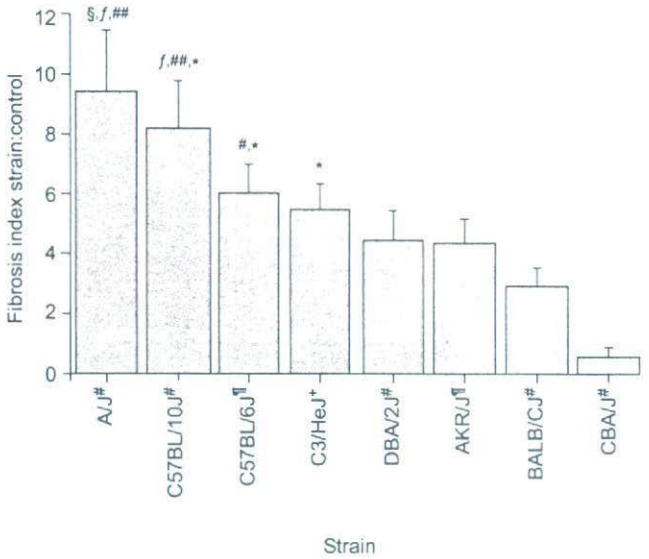

FIGURE 2. Fibrosis indices in eight strains of mice 28 days after intratracheal silica injection. Values are mean+SE. #: n=12; ¶: n=8; +: n=16; §: significantly different to AKR; f: significantly different to Balb/cJ; ##: significantly different to CBA. *: significant increase in fibrosis compared to own control $p<0.05$.

both indicators indicated significant effects of strain ($p<0.001$ and $p<0.0025$, respectively) and exposure ($p<0.0005$, $p<0.0005$), and interaction of strain and exposure effects on the mean ratio of hydroxyproline in silica-exposed groups ($p<0.0005$) and pathological fibrosis indices ($p<0.0005$) compared with TiO_2 exposed mice.

The strain distribution pattern in hydroxyproline contents among the eight strains of silica-exposed mice are shown in figure 1. The hydroxyproline content in C57BL/6J was the highest and in CBA/J was the lowest among eight strains of mice. Multiple comparisons by Tukey's test revealed significant inter-strain differences in the fibrotic response. Significant inter-strain differences were detected between C57BL/6J and Balb/cJ ($p<0.05$), and between C57BL/6J and CBA/J ($p<0.05$). The hydroxyproline content of all other silica-exposed strains, except CBA/J mice, were significantly higher than that of silica-exposed CBA/J ($p<0.05$).

The strain distribution pattern in pathological fibrosis indices among the eight strains of silica-exposed mice is shown in figure 2. The pathological fibrosis index in A/J was the highest, and that in CBA/J was the lowest among eight strains of mice. Multiple comparisons by Tukey's test revealed significant inter-strain differences in the fibrotic response. Significant inter-strain differences were detected among A/J, AKR/J, and CBA/J ($p<0.05$). The pathological fibrosis indices of all other silica-exposed strains except CBA/J mice were significantly higher than that of silica-exposed CBA/J ($p<0.05$).

As any phenotype chosen for linkage analysis investigation must be highly reproducible and quantitative [17], hydroxyproline was chosen as a marker of pulmonary fibrosis. From the study results of hydroxyproline, C57BL/6J was named as a susceptible strain and CBA/J as a resistant strain. To obtain insight about the mode of inheritance of susceptibility to silica-exposure, F1 mice derived from a cross between susceptible C57BL/6J and resistant CBA/J mice were phenotyped for their response to silica exposure. Compared with TiO_2-exposed control animals, the range of responses to silica exposure by F1 mice was between that of C57BL/6J and CBA/J progenitor mice (fig. 3). The mean response of F1 mice was significantly different from those of C57BL/6J and CBA/J mice ($p<0.05$).

A genome-wide linkage analysis was initiated to identify the chromosomal location of QTL, which control susceptibility to intratracheal silica exposure. In order to minimise experimental error [18], saline was used as a control for silica-instillation in the linkage analysis study. The first step in the analysis was to select 25 phenotypically extreme F2 responders (50 meioses), genotyped at 167 SSLP markers spaced to provide complete coverage of the mouse genome with 95% confidence [12, 14]. Interval analyses with free regression model revealed eight suggestive QTLs on chromosomes 3 (D3mit57.1), 4 (D4Mit9.1), 5 (D5Mit309.1, D5Mit277.1), 6 (D6Mit274.1), 10 (D10Mit230.1), 11 (D11Mit289.1), 14 (D14Mit98.1), and 18 (D18Mit177.1; fig. 4).

Each putative QTL was analysed further by including the F2 cohort (n=117 animals, 234 meioses). Only the chromosome 4 QTL revealed statistically significant linkage as determined empirically by permutation test (fig. 5). The amount of total trait variance explained by this QTL (at *D4Mit9.1*) was ~9%. The QTL on chromosomes 3 and 18 exceeded the threshold for suggestive linkage after the remaining F2 animals were considered in the analysis. The amount of total trait variance explained by these QTL, at *D3Mit319* and *D18Mit177.1*, was ~7 and 6%, respectively. Further interval analyses were not performed, due to the unavailability of commercial SSLPs between C57BL/6J and CBA/J.

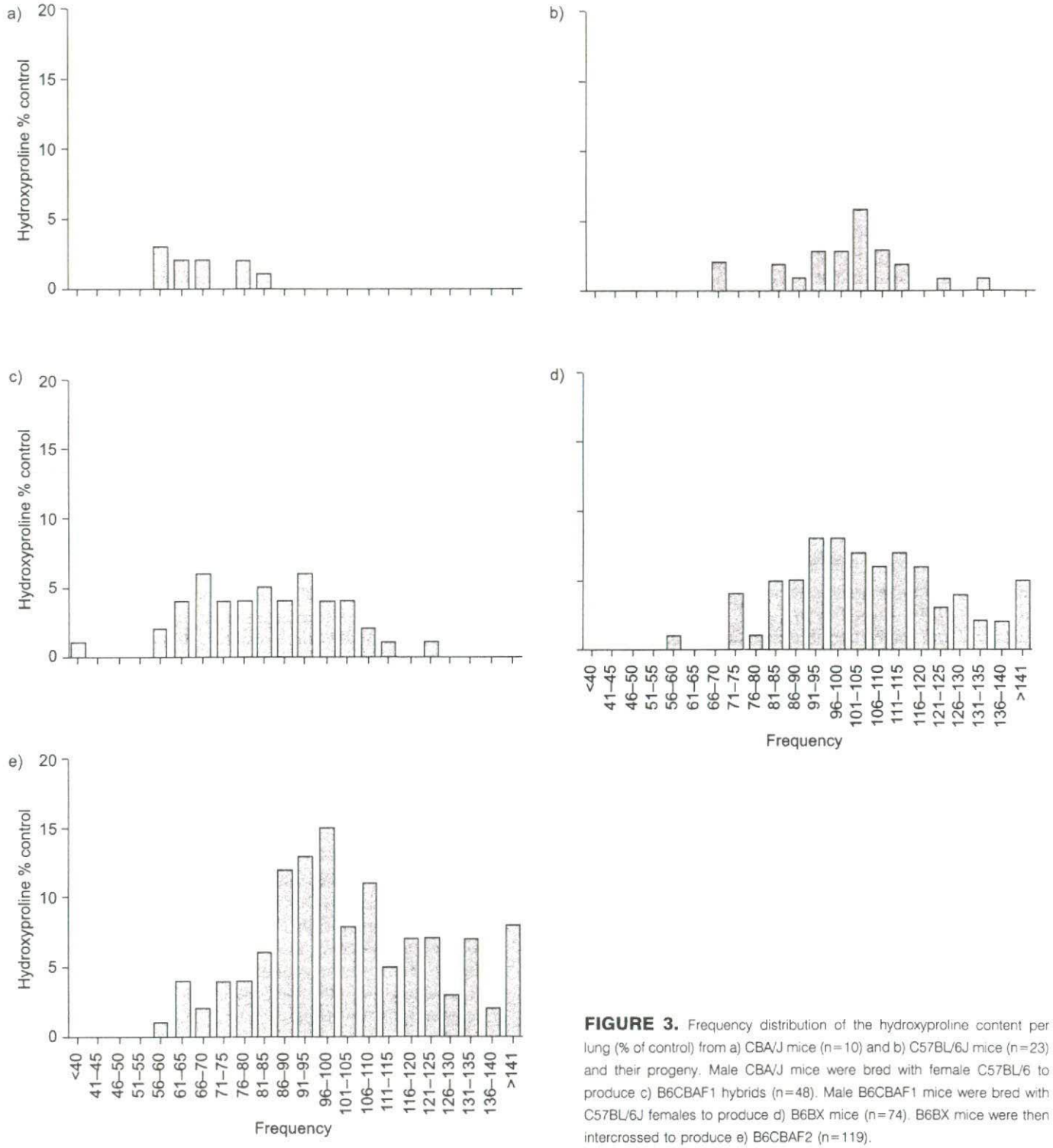

FIGURE 3. Frequency distribution of the hydroxyproline content per lung (% of control) from a) CBA/J mice (n=10) and b) C57BL/6J mice (n=23) and their progeny. Male CBA/J mice were bred with female C57BL/6 to produce c) B6CBAF1 hybrids (n=48). Male B6CBAF1 mice were bred with C57BL/6J females to produce d) B6BX mice (n=74). B6BX mice were then intercrossed to produce e) B6CBAF2 (n=119).

DISCUSSION

A clear pathological association between exposure to silica particles and silicosis has been clarified since antiquity. Epidemiological studies have also shown that duration and amount of exposure as well as content of free crystalline silica are most critical determinants of the progression of silicosis [2]. However, inter-individual variations in the development of silicosis even in the same environments have been reported. For example, specific HLA haplotype associations with silicosis have been reported in a Japanese population [3]. However, all inter-individual variability cannot be attributed solely to the major histocomaptibility complex (MHC). Therefore, genetic factors including MHC must be examined in the murine model of silicosis. Consequently, the present

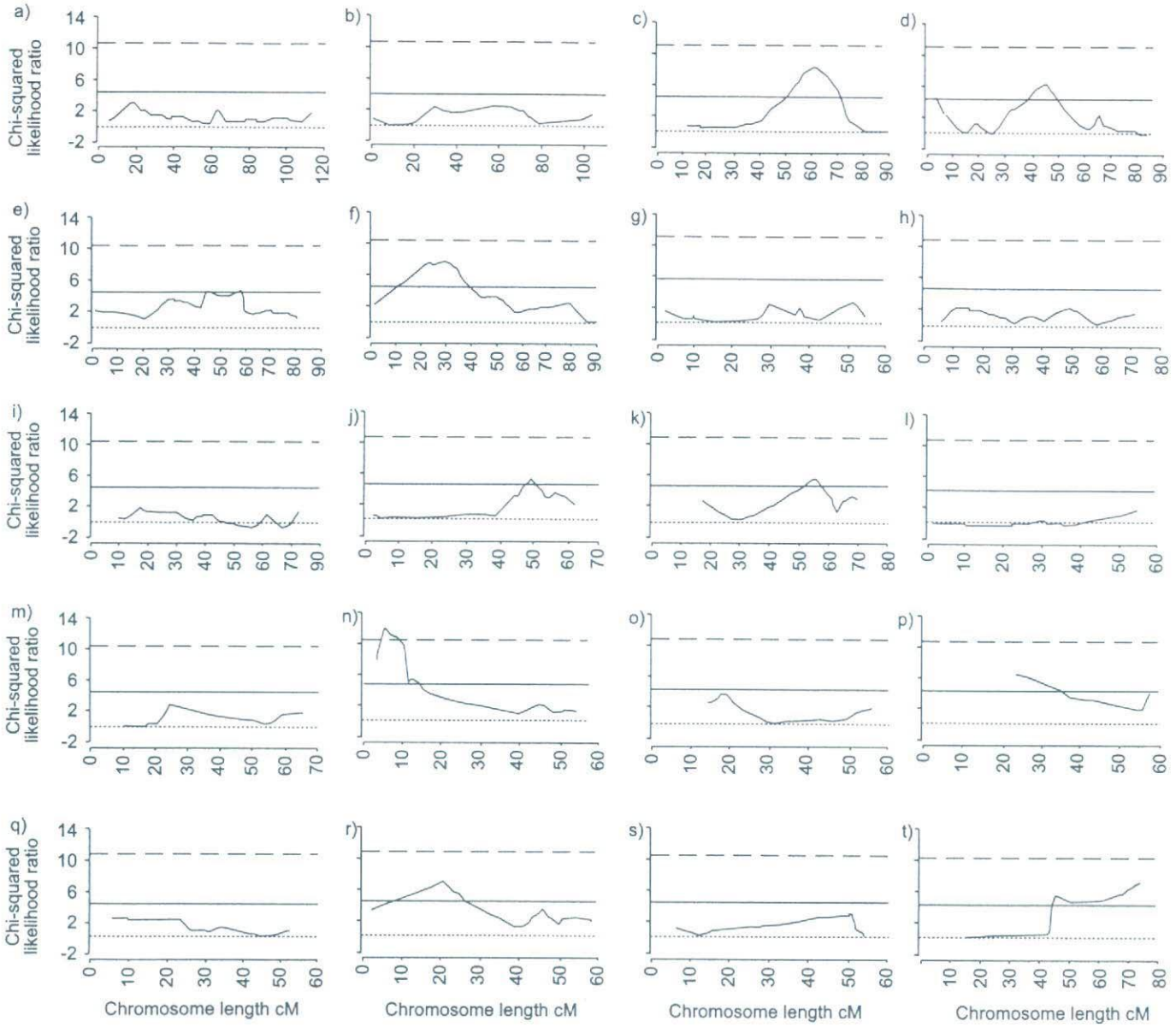

FIGURE 4. A genome-wide search for quantitative trait loci (QTL) by selective genotyping of the 25 F2 cohort (50 meiosis), *i.e.* the most extreme high and low responders to intratracheal silica-instillation. a)–f): chromosomes 1–19; t): chromosome x. cM: centimorgans; ····: 0; —: suggestive linkage threshold; – – –: significant linkage threshold. Putative QTL on chromosomes 3, 4, 6, 10, 11, 14, and 18 identified by the genome scan were further analysed with the entire F2 cohort.

authors hypothesise that genetic background contributes significantly to the variation in inflammation and pulmonary fibrosis induced by inhalation of silica in the mouse.

First, to address this question, the relative susceptibility to silica exposure in inbred strains of mice was studied. The inbreeding process results in genetic homogeneity at almost all loci, and different inbred strains of mice may be homogeneous for different alleles at the same loci. Generally, strains with greater evolutionary divergence will have a greater degree of polymorphism than strains that are closely related. Therefore, these characteristics enable investigations into genetic basis for a physiological and/or toxicological response of a phenotype. That is, if a difference in a chosen phenotype is found after a screen of a number of inbred strains to provide sufficient variation across the species, then it may be concluded that one or more loci contributes to the genetic variance observed among strains [17]. The present study evaluated fibrotic response after exposure to intratracheal silica-instillation in eight strains of mice chosen based on their differing lineage and common usage in genetic studies. The significant inter-strain variation (genetic) in the fibrotic response to silica exposure supports the hypothesis that susceptibility to silica exposure in inbred mice has a significant genetic component.

Secondly, to determine whether susceptibility to silica exposure is inherited as a dominant or recessive trait, hydroxyproline content was determined in silica-exposed B6CBAF1/J mice. Although the hydroxyproline content of B6CBAF1/J mice was different to that of silica-exposed C57BL/6J and

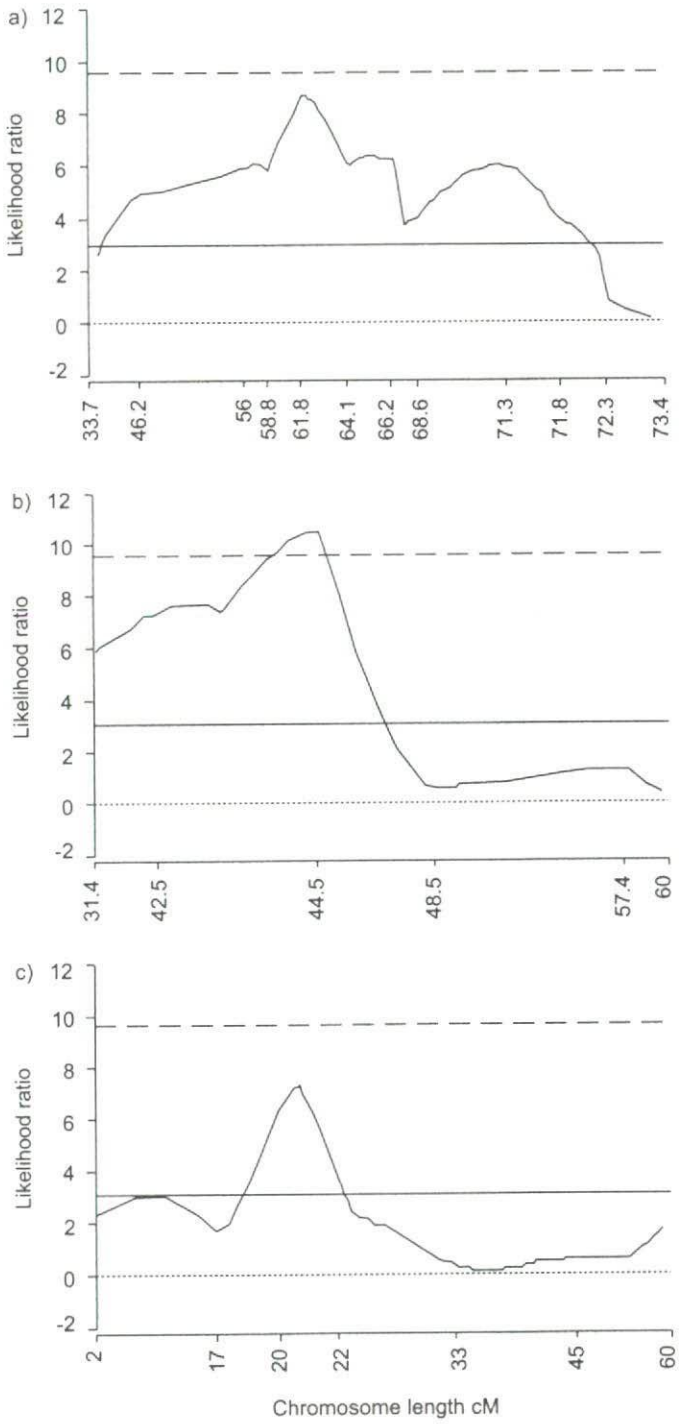

FIGURE 5. Chi-squared likelihood ratio for the association of silica-instilled, lung hydroxyproline content (% of controls) phenotype with polymorphic simple sequence length polmorphism markers on chromosomes a) 3, b) 4 and c) 18. Internal mappings were performed by simple linear regression, —: suggestive linkage threshold; - - -: significant linkage threshold.

CBA/J mice, the phenotype of F1 showed full phenotype of the dominant trait and the mode of inheritance seems to be complex in this model. Further characterisation of the mode of inheritance will need formal segregation analyses in segregated backcross and intercross populations derived from C57BL/6J and CBA/J mice as previously performed by KLEEBERGER *et al.* [18].

Thirdly, to further explore a genetic basis for susceptibility to silicosis, a QTL analysis was performed of a large F2 mice population generated from the CBA/J and C57BL/6J strains. In this study, a significant QTL for susceptibility to silicosis was identified on chromosome 4 with two suggestive QTLs also identified on chromosomes 3 and 18.

Several studies have used inbred strains of mice to identify susceptible genes for pulmonary fibrosis. HASTON and co-workers [19, 20] identified two genetic loci, chromosome 17 (MHC) and chromosome 11 in a radiation-induced lung fibrosis model. These QTL nearly overlapped QTL identified for ozone and particular matter susceptibility [19, 21], leading HASTON *et al.* [22] to propose a common genetic influence in mouse models of lung fibrosis.

In the current study, a significant QTL was identified on chromosome 4, with a peak likelihood ratio occurring at the microsatellite marker *D4Mit9.1* (located 44.5 cM distal to the centromere) and two suggestive QTLs identified in chromosomes 3 and 18. These QTL were different from other QTL in a mouse model of bleomycin- and radiation-induced lung fibrosis. The present results suggest that different mechanisms may play roles in pathophysiological mechanisms in the development of lung fibrosis. Differing from bleomycin and radiation, crystalline of silica is an inorganic dust and causes a granulomatous reaction in the lung. This factor might induce different pathophysiological mechanisms in the lung and yield different results.

There are several candidate genes within chromosome 4 QTL, including the oncogene *jun*, insulin-like growth factor binding protein-like-1 (*Igfbp-1*), phospholipase A2 activating protein *plaa*, and cyclin-dependent kinase *cdkn2a*. The oncogene *jun* has transcriptional regulatory roles with p21, and is involved in cell mitogenic responses and growth [23]. Insulin-like growth factor binding proteins (IGFBPs), as well as insulin growth factors (IGFs), have been proposed as pathogenic in lung fibrosis. Some IGFBPs work as modulating factors of IGF and have also been detected in idiopathic pulmonary fibrosis tissues [24]. Although the function of *Igfbp-1* has not been clarified with respect to the current data, it may have potential to be one of several important candidate genes. Other candidate genes, such as *plaa* and *cdkn2*, are also transcriptional factors and have important roles in cell cycle machinery. Candidate genes around the QTL on chromosome 18 include fibroblast growth factor-1 (*fgf-1*) sprouty homolog 4 (*Spry4*; Drosophilia), and pulmonary adenoma susceptibility-9 (*pas9*). Functions of *fgf-1* have been implicated in the hepatic fibrotic process [25]. *Spry4* is an intracellular fibroblast growth factor receptor antagonist, expressed in epithelial cells of foetal lung under control of a doxycycline-inducible system. As these factors are all suggested in silicosis, their function in silicosis models warrants further investigation.

In a previous study by OHTSUKA *et al.* [9], the inheritance of phenotypic traits suggests that this silicosis model is a polygenetic rather than a single genetic model. In the present study, the sum of total trait variance explained by the three

QTL is 23%. These results suggest the important contribution of genetic factors in response to instilled silica.

In conclusion, significant inter-strain variation was shown to exist in the pulmonary responses to intratracheal instillation of silica. From this, the present authors conclude that there is a significant genetic effect on fibrotic response to silica. Furthermore, the genome-wide linkage analysis of F2 identified significant quantitative trait loci for silicosis on chromosome 4 and suggestive quantitative trait loci on chromosomes 3 and 18, respectively. This is the first demonstration of candidate loci for susceptibility to silicosis. Several interesting candidate genes (*e.g. fgf, igfbpl-1*) have been observed within the regions of interest and polymorphisms within these genes need to be further analysed. Future approaches will be the comparative sequencing of the candidate genes in eight strains of mice. To refine the identified quantitative trait loci will provide an understanding of the mechanism of the host response to silica exposure and provide a potential means to identify genetically susceptible individuals who may be at risk to adverse effects of silica exposure.

REFERENCES

1 National Institute for Occupational Safety and Health. Work-related lung disease surveillance report. Publication No. 2000–105. Cincinnati (OH), DHHS (NIOSH), 1999.
2 American Thoracic Society. Adverse effect of crystalline silica exposure. *Am J Respir Crit Care Med* 1997; 155: 761–765.
3 Honda K, Kimura A, Dong RP, *et al.* Immunogenetic analysis of silicosis in Japan. *Am J Respir Cell Mol Biol* 1993; 8: 106–111.
4 Rihs HP, Lipps P, May-Taube K, *et al.* Immunogenetic studies on HLA-DR in German coal miners with and without coal worker's pneumoconiosis. *Lung* 1994; 172: 347–354.
5 Corbett E, Mozzato-Chamay N, Butterworth AE, *et al.* Polymorphisms in the tumor necrosis factor-α gene promoter may predispose to severe silicosis in black South African miners. *Am J Respir Crit Care Med* 2002; 165: 690–693.
6 Yucesoy B, Vallyathan V, Landsittel DP, *et al.* Association of tumor necrosis factor-α and interleukin-1 gene polymorphisms with silicosis. *Toxicol Appl Pharmacol* 2001; 172: 75–82.
7 Yucesoy B, Vallyathan V, Landsittel DP, *et al.* Polymorphisms of the IL-1 gene complex in coal miners with silicosis. *Am J Industrial Med* 2001; 39: 286–291.
8 Ohtsuka Y, Munakata M, Ukita H, *et al.* Increased susceptibility to silicosis and TNF-alpha production in C57BL/6J mice. *Am J Respir Crit Care Med* 1995; 152: 2144–2149.
9 Ohtsuka Y, Wang X, Saito J, Ishida T, Munakata M. Genetic linkage analysis of susceptibility to silica exposure in mice. *Am J Respir Crit Care Med* 2004; 169: A526.
10 Ashcroft T, Simpson JM, Timbrell V. Simple method of estimating severity of pulmonary fibrosis on a numerical scale. *J Clin Pathol* 1988; 41: 467–470.
11 Woessner JF Jr. The determination of hydroxyproline in tissue and protein samples containing small proportions of this amino acid. *Arch Biochem Biophys* 1961; 93: 440–447.
12 Informative markers for a cross – mouse microsatellite studies. http://www.cidr.jhmi.edu/mouse/mouse_dif.html. Date last updated: October 2005. Date last accessed: November 2005.
13 Silver LM. Mouse Genetics. Concepts and Applications. New York, Oxford University Press, 1995.
14 Manly KF, Cudmore Jr RH, Meer JM. Map Manager QTX, cross-platform software for genetic mapping. Mammalian Genome 2001; 12: 930–932. http://www.mapmanager.org/mmQTX.html. Date last accessed: November 2005.
15 Churchill GA, Doerge RW. Empirical threshold values for quantitative trait mapping. *Genetics* 1994; 138: 963–971.
16 Lander ES, Kruglyak L. Genetic dissection of complex traits: guidelines for interpreting and reporting linkage results. *Nat Genet* 1995; 11: 241–227.
17 Kleeberger SR, Ohtsuka Y. Gene-particulate matter-health interactions. *Toxicol Appl Pharmacol* 2005; 207: Suppl. 2, 276–281.
18 Kleeberger SR, Levitt RC, Zhang LY, *et al.* Linkage analysis of susceptibility to ozone-induced lung inflammation in inbred mice. *Nat Genet* 1997; 17: 475–478.
19 Haston CK, Travis EL. Murine susceptibility to radiation-induced pulmonary fibrosis is influenced by a genetic factor implicated in susceptibility to bleomycin-induced pulmonary fibrosis. *Cancer Research* 1997; 57: 5286–5291.
20 Haston CK, Wang M, Dejournett RE, *et al.* Bleomycin hydrolase and a genetic locus within the MHC affect risk for pulmonary fibrosis in mice. *Hum Mol Genet* 2002; 11: 1855–1863.
21 Ohtsuka Y, Brunson KJ, Jedlicka AE, *et al.* Genetic linkage analysis of susceptibility to particle exposure in mice. *Am J Respir Cell Mol Biol* 2000; 22: 574–581.
22 Haston C K, Zhou X, Gumbiner-Russo L, *et al.* Universal and radiation-specific loci influence murine susceptibility to radiation-induced pulmonary fibrosis. *Cancer Research* 2002; 62: 3782–3788.
23 Shaulian E, Schreiber M, Piu F, Beeche M, Wagner EF, Karin M. The mammalian UV response: c-Jun induction is required for exit from p53-imposed growth arrest. *Cell* 2000; 103: 897–900.
24 Pilewski JM, Liu L, Henry AC, Knauer AV, Feghali-Bostwick CA. Insulin-like growth factor binding proteins 3 and 5 are overexpressed in idiopathic pulmonary fibrosis and contribute to extracellular matrix deposition. *Am J Pathol* 2005; 166: 399–407.
25 Yu C, Wang F, Jin C, *et al.* Role of fibroblast growth factor type 1 and 2 in carbon tetrachloride-induced hepatic injury and fibrogenesis. *Am J Pathol* 2003; 163: 1653–1662.